ACCSCIENCE PUBLISHING

International Journal of Bioprinting

ACCEPTED PAPER · MAIN TEXT

Intelligent 3D bioprinting platforms for complex bone-tissue interfaces: Mechanisms, biofabrication, and regenerative applications

Article ID: IJB026350370

Citation: Cui X, Xue P, Wei W, Liang Z, Zhou T, Wang S. Intelligent 3D bioprinting platforms for complex bone-tissue interfaces: Mechanisms, biofabrication, and regenerative applications. *Int J Bioprint*. 2026. doi: 10.36922/IJB026350370

AccScience Publishing
REVIEW ARTICLE
Volume X Issue X (2026)
doi: 10.36922/IJB026350370

Intelligent 3D bioprinting platforms for complex bone-tissue interfaces: Mechanisms, biofabrication, and regenerative applications

Running title: Intelligent 3D bioprinting for bone interfaces

Xiangran Cui[1,2†], Pan Xue[3†], Wei Wei[1,2], Zhaoyu Liang[4*], Tingting Zhou[1*], and Shixuan Wang[1,2*]

[1]Liaoning University of Traditional Chinese Medicine, Shenyang 110847, Liaoning Province, China
[2]Department of Orthopedic, Second Affiliated Hospital of Liaoning University of Traditional Chinese Medicine, Shenyang, Liaoning, China
[3]Department of Traditional Chinese Medicine, Dazhou Vocational College of Chinese Medicine, Dazhou, 635000, Sichuan, China
[4]Department of Orthopedics, First Hospital of China Medical University, Shenyang, Liaoning, China

[†]*These authors contributed equally to this work.*

***Corresponding authors:**
Zhaoyu Liang (yzl202504@foxmail.com)
Tingting Zhou (1297713226@qq.com)
Shixuan Wang (wangshixuan99@126.com)

Citation: Cui X, Xue P, Wei W, Liang Z, Zhou T, Wang S. Intelligent 3D bioprinting platforms for complex bone-tissue interfaces: Mechanisms, biofabrication, and regenerative applications. *Int J Bioprint*. 2026. doi: 10.36922/IJB026350370

Received: August 1, 2026
Revised: August 25, 2026
Accepted: September 11, 2026
Published online: September 16, 2026

Abstract

Bone-tissue interfaces—including both anatomically-defined structures (osteochondral, tendon-to-bone, ligament-to-bone) with characteristic compositional gradients, and functional biological interactions (bone-immune, bone-vascular, bone-nerve that regulate systemic regenerative processes)—represent critical repair targets. Traditional strategies fail due to mechanical mismatch and poor integration. 3D bioprinting enables precise, patient-specific construction of multi-gradient scaffolds through co-deposition of diverse biomaterials and cell types, transcending structural mimicry to coordinate multilineage differentiation and microenvironmental regulation. This review systematically synthesizes advances in six interface categories, moving beyond study-by-study description to comparative analysis. We distinguish structural approaches (pore regulation, fiber reinforcement, microchannels) that primarily improve biomimicry from bioactive strategies (growth factors, hypoxia, immunomodulation) that direct cell fate, clarify experimental validation levels (in vitro vs. animal models), and delineate appropriate clinical scenarios. Key bottlenecks include insufficient deep vascularization, temporal immune regulation mismatches, and mechanical integration unpredictability. Future directions encompassing organ-on-chip integration, AI-driven personalization, and organoid-inspired self-organization are outlined. 3D bioprinting emerges as a unified platform for both anatomical interface reconstruction and functional biological orchestration in regenerative medicine.

Keywords: 3D bioprinting; Bone-tissue interfaces; Tissue engineering; Regenerative medicine; Bioactive materials

1. Introduction

Bone, as the most critical structural support of the human body, relies on its functionality through interactions with various soft tissues such as blood vessels, nerves, tendons, cartilage, and ligaments[1-4]. These bone-tissue interfaces are not simple boundaries, but rather complex transitional zones with distinct layered or gradient features, where structure, composition, and mechanical properties transition continuously along the interface to accommodate stress transmission and functional transition between different tissues[4-7]. However, factors such as trauma, disease, infection, or tumor resection can readily damage these critical interfaces, and their intrinsic repair capacity is extremely limited, often failing to achieve complete functional regeneration and frequently ending in fibrous scar tissue formation[8,9]. Millions of people worldwide suffer annually from bone-tissue interface-related conditions such as tendon tears, ligament ruptures, osteochondral defects, and peripheral nerve injuries[10,11]. These injuries not only cause patients chronic pain, functional impairment, and reduced quality of life, but also impose substantial treatment and rehabilitation costs, placing a heavy economic and social burden on individuals and society[12,13]. Current clinical treatments primarily include direct surgical repair, graft implantation, and microfracture surgery[14,15]. However, these conventional approaches are broadly limited by issues such as donor site complications, poor graft-host tissue integration, mechanical strength mismatch, high re-tear rates, and an inability to effectively promote vascularization and innervation. These shortcomings highlight the urgent need to develop innovative strategies and technologies for structural remodeling and functional reconstruction of bone-tissue interfaces[16,17].

3D bioprinting technology, centered on additive manufacturing, offers unprecedented opportunities for addressing the challenge of repairing bone-tissue interface connections[18-20]. In the context of this review, 3D bioprinting is used in a functional sense: it includes printing workflows that are intended to deliver either (i) spatially organized cells (cell-laden/bioink printing) during fabrication, or (ii) biologically active microenvironments (e.g., immunomodulatory or angiogenic architectures) where the printed construct is explicitly designed as an ‘interactive’

therapeutic platform for bone-associated interface regeneration. Therefore, we further categorize the studies summarized here into three groups: (1) direct bioprinting, i.e., cell-laden printing in which cells are embedded/co-printed or positioned during the printing process (e.g., extrusion/electrospinning/DLP-based cell-containing bioinks, aspiration-assisted printing with cell spheroids); (2) conventional additive manufacturing, i.e., 3D printed scaffold architectures that regulate cells in vivo primarily through structural/chemical cues (e.g., pore size–mediated osteoimmune modulation) without explicit cell dispensing as part of the printing step; and (3) post-printing cell seeding approaches, where the scaffold is fabricated first and cells are subsequently seeded to probe biological outcomes. When groups (2) and (3) are included, this is done only when the printed architecture is used to mechanistically inform interface regulation in vivo (e.g., immune polarization, angiogenic invasion, or long-term integration), rather than to replace cell-laden printing as the central focus of the review.

This technology can precisely construct patient-specific three-dimensional scaffolds based on medical imaging data (such as CT and MRI), thereby overcoming the limitations in achieving structural complexity and patient-specific personalization[21,22]. 3D bioprinting demonstrates significant advantages in bone-tissue interface repair: it enables precise control over the scaffold's macroscopic geometry and microscopic pore architecture, thereby accurately mimicking the hierarchical structure of natural interface gradients, including continuous transitions in material composition, porosity, and mechanical strength[23-25]. Meanwhile, its multi-material and multi-cell printing capabilities allow the simultaneous deposition of different types of biomaterials (such as rigid bone-phase materials and flexible soft-tissue hydrogels) as well as multiple cell types (such as osteoblasts, chondrocytes, tenocytes, vascular endothelial cells, and neural cells) within a single construct, thereby recreating the complex heterogeneity of natural interfaces[26-28]. This enables the construct to better guide tissue growth, promote cell differentiation, and form closer connections with host tissue. However, despite the tremendous breakthroughs 3D bioprinting has achieved in structural biomimicry, mere structural replication is often insufficient to achieve

complete functional regeneration and long-term interface integration[29-32]. Current challenges lie primarily in how to further enhance the biological activity and biofunction of bioprinted constructs, effectively promote cell survival and function, accelerate vascularization and nerve regeneration, and regulate the complex in vivo microenvironment to avoid adverse immune responses and fibrosis, ensuring seamless biological and mechanical integration between the construct and host tissue[33-35]. These issues represent critical bottlenecks that 3D bioprinting technology urgently needs to overcome, necessitating for the introduction of more bioinductive strategies.

To further enhance the capability of 3D bioprinting in bone and tissue interface repair, combining 3D bioprinting technology with various bioactive materials (such as bioceramics, bioglass, bioactive polymers, natural macromolecules, as well as growth factors and cytokines) has become a research hotspot in the field of biomedical engineering[36-38]. The introduction of these bioactive materials serves not merely as simple structural support, but more importantly, they can actively participate in the tissue regeneration process by releasing bioactive ions, inductive growth factors, or directly regulating cell behavior[39-41]. Leveraging the precise positioning capability of 3D bioprinting, it is possible to construct intelligent biological scaffolds that can both simulate the mechanical gradients and structural characteristics of natural interfaces and provide continuous bioinductive signals[42-44]. This strategy can promote coordinated growth and differentiation of distinct cell types, including osteocytes, osteoblasts, chondrocytes, tenocytes, neuronal cells, and vascular endothelial cells, accelerating the formation of functional interfaces. For example, bioprinted scaffolds loaded with vascular endothelial growth factor can significantly promote vascular ingrowth, while scaffolds containing nerve growth factor effectively facilitate nerve regeneration[45-47]. Furthermore, by carefully designing the composition of bioactive materials, it is even possible to regulate the local immune microenvironment, polarizing macrophages toward a pro-repair phenotype, thereby alleviating inflammatory responses and promoting tissue repair and integration[48-50]. This organic combination of 3D bioprinting and bioactive materials establishes a novel pathway for achieving precise, efficient, and functional repair of complex bone and tissue interfaces[51,52].

We searched the web of sci database for relevant articles published in the past 10 years (2016-2026), using bone, interface, bioprinting as keywords. We only retained original research articles, excluding reviews, conferences, and other types of articles. Table 1 is a summary of all original research papers.

In this review, we consider "bone-tissue interfaces" to encompass two distinct categories. Anatomically-defined interfaces (bone-cartilage, bone-tendon, bone-ligament) are discrete transitional zones with characteristic gradients in composition, mechanics, and cell types, where the interface itself occupies a specific spatial region. Functional biological interactions (bone-immune, bone-vascular in the context of physiological regulation rather than structural coupling) refer to dynamic crosstalk between bone and other tissues or cell types that influence regeneration without necessarily constituting a localized anatomical boundary. Both categories require spatial organization and temporal coordination but differ in design priorities: anatomically-defined interfaces prioritize structural gradient reconstruction, while functional interactions emphasize microenvironmental regulation. This unified framework acknowledges that modern bone-tissue interface engineering must address both structural mimicry and dynamic biological control.

This review aims to provide a comparative and mechanistic synthesis of intelligent 3D bioprinting for bone-associated tissue interfaces, rather than serving as a simple catalog of interface-specific studies. Although previous reviews have separately discussed osteochondral regeneration, tendon-to-bone healing, musculoskeletal interface engineering, and 3D bioprinting technologies, important questions remain insufficiently addressed across these topics: how interfacial gradients are rationally designed, how compositional transitions and spatial cell organization are coordinated, how vascular and neural integration can be synchronized with tissue maturation, and how immune responses are temporally modulated to support durable interface regeneration (Fig 1.).

Accordingly, the rationale for discussing bone-cartilage, bone-vessel, bone-nerve, bone-tendon, bone-ligament, and bone-immune interfaces within the same review lies in their shared biological and engineering principles. These systems all require

hierarchical transitions in composition, mechanics, and cellular microenvironment, and all face the same translational challenge of balancing structural mimicry with long-term functional adaptation. In this sense, the academic contribution of the present review is to move beyond a tissue-by-tissue description and instead summarize the common design logic of printed interfaces, including gradient architecture, multicellular spatial organization, bioactive signal delivery, vascular–neural coupling, osteoimmune regulation, and mechanically dynamic integration **(Table 1)**.

By organizing the discussion around these shared scientific questions, this review highlights what has already been established in the existing literature and, more importantly, what remains unresolved for future research and clinical translation. The comparative framework presented here is intended to distinguish this work from prior reviews that primarily focus on a single tissue interface or on printing methods alone, while providing a more unified perspective for the development of multifunctional bioprinted constructs.

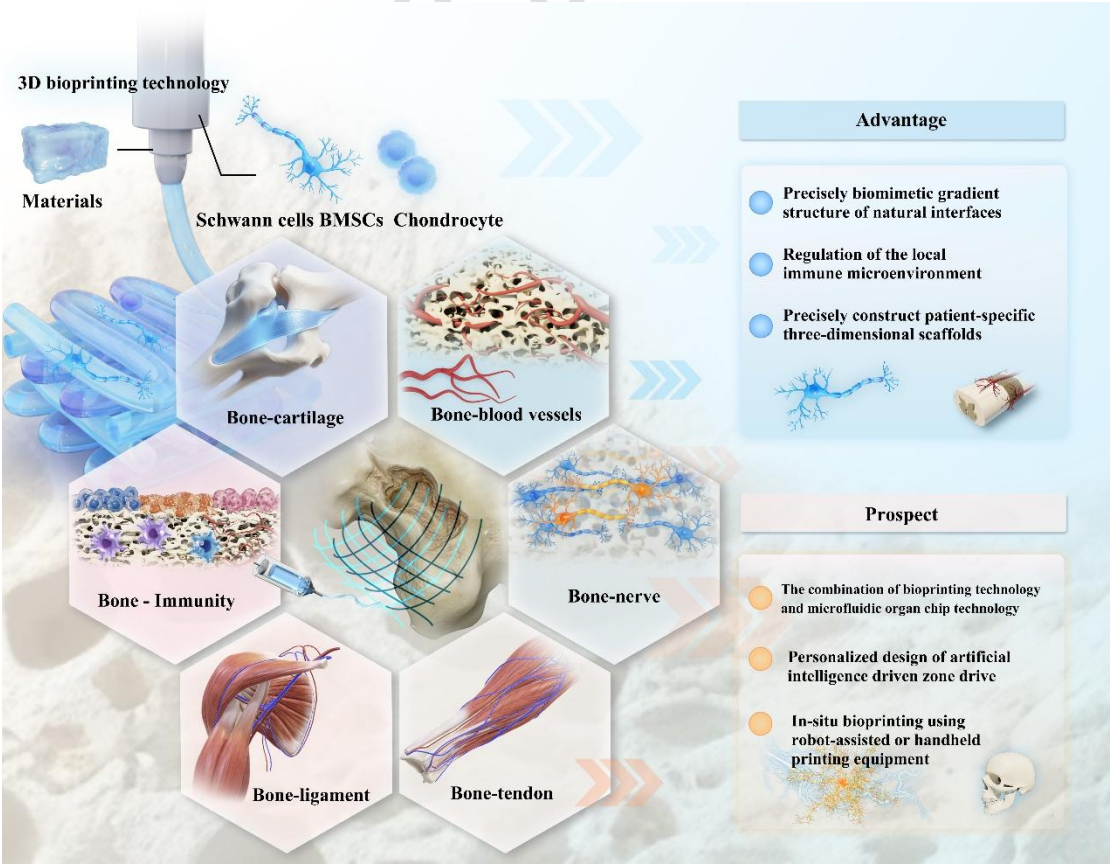

Figure 1. 3D bioprinted bone tissue interface diagram. (A) By using 3D bioprinting technology, the bone-cartilage interface, bone-vascular interface, including, anatomically defined interfaces (bone-cartilage, bone-tendon, bone-ligament) and functional biological interactions (bone-immune, bone-vascular) (B) At the same time, the main advantages of 3D bioprinting technology are summarized: it can accurately simulate the gradient structure of natural tissue interface, regulate local immune microenvironment, and construct patient-specific three-dimensional scaffolds. (C) The future development directions in this field include the combination of bioprinting technology and microfluidic organ chip technology; Personalized design of artificial intelligence driven zone drive; In-situ bioprinting using robot-assisted or handheld printing equipment.

Table 1. 3D bioprinting-related strategies for complex bone-tissue interface regeneration (including cell-laden bioprinting, structural 3D printed scaffolds, and post-printing cell seeding).

Bone interface	species	Cell type	Bioprinting method	Biomaterial	Summary	Ref
bone-cartilage	human	ADMSCs	Extrusion-based printing	Me-HA/HAp	HAp and hypoxia modulate ADMSC chondrogenesis/hypertrophy in 3D bioprinted constructs, enhancing interface integration for orthopedic repair.	53
	Equine	ACPCs	Extrusion-based printing	P-CL-MA	Integrating extrusion and MEW creates a reinforced osteochondral plug with enhanced hydrogel-ceramic adhesion and biomimetic mechanical properties.	54
	Human	ADSCs	Aspiration-assisted bioprinting	Alginate-CaCl2	Aspiration-assisted bioprinting (AAB) fabricates scaffold-free, layered osteochondral interfaces using human ADSC spheroids for tissue engineering and disease modeling.	55
	Porcine	BMSCs/Chondrocytes	Extrusion-based 3D printing	PLA、PLGA、RGD-γ alginate	3D printed fiber-reinforced bi-phasic templates successfully regenerate subchondral bone and articular cartilage in caprine osteochondral defects.	56
	Human	ADSCs	Hybrid bioprinting	Alginate-CaCl2	3D-bioprinted miR-transfected ADSC spheroids form layered, scaffold-free osteochondral interfaces with enhanced differentiation for regenerative medicine.	57
	Human	C28/I2	Extrusion-based bioprinting	PLA/Alginate	3D-bioprinted multi-zonal and gradient PLA scaffolds with concurrent cell-laden hydrogels	21

				provide biomimetic hierarchical structures for osteochondral regeneration.	
Human	ADSCs	Embedded bioprinting	GelMa /α-TCP	Freeform "bone-ink" printing within tunable microgel suspensions enables one-pot biofabrication of hierarchical, multiphasic osteochondral constructs.	58
Human	hBMSCs	Aspiration-assisted bioprinting	Alg-Tyr /CMC-Tyr/Gel	Aspiration-extrusion bioprinting using in situ crosslinked tyramine-modified hydrogels creates MSC-laden gradient structures for functional biomimetic osteochondral interface engineering.	26
Human	Human chondrocytes	Extrusion-based bioprinting	PCL/HA/Alg/A	Biphasic 3D bioprinted PCL-hydroxyapatite and alginate-gelatin composite scaffolds promote functional cartilage-bone interface regeneration with enhanced stability and bioactivity.	59
Rabbit	ACPCs	Two-channel extrusion-based bioprinting	GelMA/AlgMA	Bioprinted anisotropic bicellular hydrogels achieve synchronized osteochondral regeneration by orchestrating spatial cell differentiation and harmonious tissue-vessel crosstalk.	60
Rat	BMSCs	Digital Light Processing	bdECM-MA	3D-bioprinted graded scaffolds with tissue-specific dECM coatings promote functional tendon-to-bone enthesis regeneration and enhance biomechanical healing.	61
Human	BMSCs	Extrusion-based bioprinting	GelM -SA/HA-EW	TCOS scaffolds bioprinted via MAPM-BPS promote osteochondral repair by coordinating	30

					subchondral angiogenesis and vascular-blocking interface layers.	
	Rat	BMSCs	Digital Light Processing	Col II MA/HAMA/HAP	DLP-bioprinted BioGraOstO scaffolds with graded bioinks facilitate integrated osteochondral repair through region-specific differentiation in rat models.	62
	Rat	BMSCs	Extrusion-based 3D bioprinting	GelMA-Alginate/SA-CeMOF-BTO	Biphasic scaffolds with CeMOF@BTO synergize piezoelectric stimulation and ROS modulation to enhance ultrasound-driven osteochondral regeneration and interface reconstruction.	63
	Human	hMSCs	Extrusion-based 3D bioprinting	GelMA/Alginate/SA-PCL	Dual-gradient 3D-printed scaffolds integrate mechanical and metabolic cues for osteochondral regeneration and osteoarthritis modeling using human MSC spheroids.	64
Bone-blood vessels	Human	hMSCs	Fused Deposition Modeling	PLA/nHA	nHA-functionalized 3D bioprinted scaffolds with interconnected microvascular channels enhance hMSC osteogenesis and HUVEC growth for vascularized bone regeneration.	65
	Human	hMSCs	Direct-writing bioprinting	GelMA/VEGF/Silicate nanoplatelets	Bioprinted bone constructs with perfusable lumens and silicate-loaded GelMA promote hMSC osteogenesis and HUVEC-mediated vascularization.	66
	Human	WJMSCs	Extrusion-based bioprinting	PCL/CS/PDACS	3D bioprinted PDACS/PCL scaffolds with WJMSCs and HUVEC-laden hydrogel promote	67

				coupled osteogenesis and angiogenesis for complex bone regeneration.	
Human	hMSCs/HUVECs	Extrusion-based bioprinting	PCL/Fibrin/Gelatin	3D bioprinted osteon-like PCL/fibrin scaffolds with HUVECs and hMSCs enhance neovascularization and mechanical strength for bone regeneration.	68
Human	ASCs	Drop-on-demand (DoD) bioprinting	Fibrinogen/Gelatin-HA/Glycerol、HAp	Extrusion and drop-on-demand bioprinting of ASCs and HUVECs create prevascularized bone constructs that successfully form vessels and bone in vivo.	69
Human	hMSCs	Extrusion-based bioprinting	Gelatin/nHA/Genipin/Pluronic F-127	3D bioprinted gel-nHA scaffolds with hMSCs and HUVECs create vascularized bone models where endothelial cells enhance osteogenic maturation.	70
Human	HUVECs	Dual-ink 3D printing	CaP/Alginate/GelMA	Dual-ink bioprinting integrates CaP fibers and microchannels to support vascularization and hMSC differentiation into pericytes for bone regeneration.	70
Human	hBMSCs，HUVECs	Extrusion-based bioprinting	GD-Alginate/HA/PCL-nHA	Bioprinted fibrin-hMSC-HUVEC scaffolds enhance vascularization and bone regeneration in rat femoral defects after in vitro maturation.	71
Rabbit	BMSCs，EPCs	xtrusion-based 3D bioprinting	PCL/Gelatin/Fibrinogen/HA/Glycerol/Pluronic F-127	3D bioprinted osteon-mimetic PCL scaffolds incorporating BMSCs and EPCs enhance vascularized bone regeneration through hierarchical biomimetic microchannels.	72

	Human	HUVECs，MC3T3-E1	oaxial extrusion-based 3D bioprinting	GelMA/Alginate/Gelatin/ HAp	Coaxial 3D bioprinted osteon-like core-shell scaffolds enhance vascularization and osteogenesis compared to homogeneous structures for bone regeneration.	73
	Human	NSCs，HUVECs，L6 cells	3D bioprinting	Gelatin/GelMA/LCS	Inorganic-biomaterial/NSC neural constructs promote versatile regeneration across CNS, bone, and muscle through enhanced neural induction and functional recovery.	74
	Rat	Human EPCs	Coaxial 3D bioprinting	Atelocollagen/Alginate/Pluronic F-127/MSNs	3D bioprinted SR1-loaded collagen-MSN scaffolds promote CD34+ cell-mediated angiogenesis and bone regeneration in critical-sized defects.	28
	Rabbit	ACPCs，BMSCs	Extrusion-based bioprinting	GelMA/AlgMA	3D bioprinted living cell-based bilayered hydrogels promote biomimetic osteochondral unit remodeling and repair through spatiotemporal tissue crosstalk.	60
	BALB/c nude mice	HUVECs	DLP bioprinting	GDMA/LAP/Tartrazine	NOVA bioprinting integrates modular assembly to create vascularized tubular bone organoids, coupling angiogenesis and osteogenesis for functional defect repair.	75
Bone-nerve	Mouse	MC3T3-E1，PC12	Extrusion bioprinting	OPF/Gelatin/PEGDA/Irgacure 2959	Bioprinted OPF-gelatin bioinks support excellent viability and proliferation of bone and nerve cells for complex tissue restoration.	76
	Rat	BMSCs，SNs/DRG neurons，Schwann cells	Air extrusion-based 3D bioprinting	GelMA/AlgMA/Laponite/ NGF	Bioprinted NGF@Lap constructs promote bone regeneration by mimicking the ossification	77

				center and enhancing neurovascular network-mediated osteogenesis.	
Murine	BMSCs，PC12 cells	Additive-lathe 3D bioprinting	GelMA/PEGDA	Multi-nozzle additive-lathe bioprinting fabricates BMSC-laden bilayered conduits, balancing mechanical strength and biocompatibility for effective peripheral nerve repair.	78
Rat	BMSCs, Schwann cells	Extrusion-based multi-channel 3D bioprinting	GelMA/CS/LAP	Bioprinted neural-bone constructs using calcium silicate nanowires enhance osteogenesis and innervation for biomimetic bone regeneration.	79
Rat	PC12 cells,BMMCs	Extrusion-based 3D bioprinting	GelMA/SA/Lap/NP@Eth	Bioprinted nifedipine-loaded scaffolds promote bone regeneration by inhibiting sympathetic nerve-mediated catecholamine release and enhancing osteogenesis.	80
Rat	BMSCs, Schwann cells,EPCs	Extrusion-based 3D bioprinting	GelMA-SilMA/SC-exos	Bioprinted SC-exos-laden constructs enhance bone regeneration by promoting let-7c-5p-mediated osteogenesis, vascularization, and innervation, simulating nerve-bone crosstalk.	81
Human	BMSCs,HUVECs	Extrusion-based 3D bioprinting	GelMA/PEGDA/MSNs-PRN	Bioprinted scaffolds releasing CGRP and propranolol enhance bone repair by modulating neuro-bone crosstalk and promoting vascularized osteogenesis.	82
Human	HUVECs, hpMSCs, PC-12 cells	Extrusion-based 3D bioprinting	GelMA/LMS/LAP	Bioprinted pre-angiogenic silicate scaffolds promote "vascular-innervated" bone regeneration by synergistically enhancing	83

					simultaneous vascularization, innervation, and osteogenesis.	
	Rat	NSCs	Extrusion-based 3D bioprinting	LCS/GelMA	3D bioprinted LCS-NSC scaffolds promote CNS, bone, and muscle regeneration via PI3K-AKT-mediated neuronal maturation and neural modulation.	74
	Rat	BMSCs,RSC96	Extrusion-based 3D bioprinting	GelMA/mPGA/AC-PEG-BP/AC-PEG-NP	3D bioprinted neuro-bone constructs with mimetic peptides promote bone and nerve regeneration by modulating BMSC-RSC96 crosstalk and signaling pathways.	84
	Rat	DRG neurons,EPCs	Extrusion-based 3D bioprinting	GelMA/LAP/PDLLA	Bioprinted piezoelectric DRG scaffolds enhance neuro-vascularized bone repair via ultrasound-triggered CGRP secretion, establishing a functional "sensor-effector" interoception circuit.	85
bone-tendon	Human	MSCs	Multi-head tissue/organ building system	PCL/PLGA/b-TCP	3D bioprinted MSC-seeded sleeves enhance tendon-to-bone healing in rabbit ACL reconstruction.	86
	Rat	Endogenous progenitor cells	Extrusion-based 3D printing	PLGA/COL-I	3D-printed scaffolds with spatiotemporal growth factor delivery promote integrative tendon-to-bone healing via endogenous progenitor cell recruitment.	87
	Mouse	BALB/3T3	Pneumatic extrusion-based bioprinting	eADF4(C16), FAP	Comprehensive review of 3D bioprinting for bone-tissue interface regeneration, highlighting	88

					gradient biomaterials, multicellular strategies, and future clinical potential.	
	Human	hUCMSCs	Microfluidic-based 3D bioprinting	PLGA/RGD-alginate/Fibrinogen	Bioprinted constructs with layer-specific growth factors guide stem cell differentiation for functional rabbit rotator cuff enthesis regeneration.	89
	Human	hBMSCs	Extrusion-based 3D bioprinting	PCL/PLGA/HA/dECM	3D-bioprinted dECM-coated graded scaffolds promote functional tendon-to-bone enthesis regeneration via guided regional differentiation in a rabbit model.	90
	Rabbit	BMSCs，TSPCs	Multi-channel extrusion-based 3D bioprinting	GelMA/MS	3D-bioprinted multicellular scaffolds with Mo-silicate bioceramics mimic interface gradients to promote integrated tendon-to-bone regeneration via multi-lineage differentiation.	91
	Human	hASCs	3D bioprinting with a core-shell nozzle system	TdECMA/BdECM/HA/PVA	Core-shell bioprinted dECM scaffolds with gradient bioinks guide stem cells for functional rotator cuff enthesis regeneration in rabbits.	92
	Rabbit	hASCs	Core-shell nozzle-assisted 3D bioprinting	Collagen/CMA-beads	Bioprinted graded constructs with BMP-2-loaded CMA-beads accelerate bone-to-tendon interface regeneration and functional healing in rabbit rotator cuff models.	93
bone-Immunity	Rat	BMMs	Dual-channel bioprinting	GelMA/HAMA/Alginate/GO	Dual-channel bioprinted scaffolds encapsulating BMSCs and BMMs promote bone repair by modulating early immune responses and late osteogenic differentiation.	50

	Mouse	RAW 264.7	Pneumatic extrusion 3D printing	PCL/PEG/HA	3D-printed PCL/PEG/HA scaffolds with 600μm pores optimize bone repair by reducing foreign body response and modulating macrophage polarization.	94
	Rat	rBMSCs，BMDMs	Extrusion-based 3D printing	GelMA/Lap/Apt19s	3D-printed Apt19s-functionalized GelMA/Laponite scaffolds promote in situ bone regeneration by recruiting BMSCs and modulating osteoimmunology via AMPK/mTOR signaling.	95
	Mouse	RAW 264.7，rBMSCs	Extrusion-based 3D bioprinting	GelMA/LUT/ZIF-8	3D bioprinted LUT@ZIF-8/GelMA scaffolds promote bone repair by delivering BMSCs and modulating osteoimmunology via sustained luteolin and zinc release.	96
bone-ligament	Human	hPDLFs，hOBs	Pneumatic extrusion 3D bioprinting	Gel-MA/HAp/MNPs	3D-bioprinted multi-cellular PDL-AB microtissue models simulate human periodontal biointerfaces for studying disease pathogenesis and drug interactions under microfluidics.	97
	Human	Human ACL fibroblasts	Modular scaffold-free spheroid fusion	Scaffold-free	Fusion of human ACL and osteogenic hMSC spheroids creates scaffold-free, graded enthesis microtissues for repair modeling and mechanobiology studies.	98

Abbreviations: AAB: Aspiration-assisted bioprinting; ACL: Anterior cruciate ligament; ACPCs: Articular cartilage progenitor cells; ADMSCs: Adipose-derived mesenchymal stem cells; ADSCs: Adipose-derived stem cells; Alg: Alginate; AlgMA: Alginate methacryloyl; ASCs: Adipose-derived stem cells; BMP-2: Bone morphogenetic protein 2; BMMs: Bone marrow-derived macrophages; BMSCs: Bone marrow-derived mesenchymal stem cells; bdECM-MA: Bone decellularized extracellular matrix methacryloyl; BTO: Barium titanate oxide; CaP: Calcium phosphate; CeMOF: Cerium metal-organic framework; CGRP: Calcitonin gene-related peptide; CMC-Tyr: Carboxymethyl cellulose tyramine; COL-I: Collagen type I; Col II MA: Collagen II methacryloyl; CS: Calcium silicate; dECM: Decellularized

extracellular matrix; DLP: Digital light processing; DRG: Dorsal root ganglion; eADF4(C16): Engineered spider silk protein; EPCs: Endothelial progenitor cells; FAP: Fibroblast activation protein; FBR: Foreign body reaction; GD-Alginate: Gelatin-dopamine alginate; Gel: Gelatinα-TCP: Alpha-tricalcium phosphate; β-adrenergic: Beta-adrenergic.

2. Bioprinting methods

2.1 Extrusion-based bioprinting

Extrusion-based 3D bioprinting is one of the most widely used bioprinting technologies. It works by applying external pressure (such as air pressure, piston, or screw drive) to extrude viscous bioinks from a fine nozzle, forming continuous fibrous structures that are then deposited layer by layer to construct a three-dimensional object[99-101]. This method is particularly suitable for printing bioinks with a wide range of viscosities, including composite hydrogels such as alginate, gelatin, collagen, hyaluronic acid, Pluronic, and decellularized extracellular matrix[102-104]. These materials can carry exceptionally high cell densities (up to 10^8 cells/mL) and can simultaneously incorporate microparticles, nanoparticles, or growth factors[105,106].

The limitations of extrusion-based bioprinting include its relatively limited printing resolution, with nozzle diameters and print line widths typically ranging from 100 micrometers to 500 micrometers, making it difficult to achieve sub-micron fine structures. Additionally, the printing speed is relatively slow, and cells may experience shear stress[107,108]. Conversely, its unique advantage lies in its ability to process diverse and highly viscous bioinks, printing macroscopic structures with good mechanical strength and dimensional stability, and achieving high cell viability (often over 90% after optimization). In bone-tissue interface bioprinting applications, extrusion-based technology demonstrates excellent compatibility. It can precisely co-print materials with different mechanical properties and biological activities, for example, accurately depositing hard bioinks containing hydroxyapatite (simulating bone) alongside cell-rich elastic hydrogels (simulating soft tissue) in a spatially controlled manner[109,110]. This allows for the simulation of complex transitions in natural interfaces through gradient structures, thereby promoting effective integration and functional regeneration between tissues[111,112].

Extrusion-based bioprinting technology is continuously innovating, with various emerging derivative methods appearing to enhance its performance and application scope. Among these, microfluidic extrusion bioprinting integrates microfluidic

channels within the printhead, enabling precise mixing of multiple bioink precursors or cell suspensions before extrusion[113,114]. This enables the real-time generation of complex biological fibers with core-shell structures, hollow fibers, or multi-channels, greatly enhancing control over the microscopic structure of printed materials[115,116]. Melt Electrowriting (MEW) technology, although typically employed for thermoplastic polymers rather than direct cell encapsulation, combines the principles of extrusion and electrospinning[117,118]. It can precisely deposit molten polymer fibers with sub-micron accuracy (down to a few hundred nanometers), offering considerable potential for constructing cell scaffolds with high porosity and mechanical strength, which can then be seeded with cells[119-121]. Furthermore, In-situ bioprinting is gaining increasing attention, with researchers developing portable or robotic arm-assisted extrusion systems for directly printing tissue patches inside patients during surgery, such as repairing cartilage or skin damage[122,123]. This approach requires bioinks to cure rapidly and maintain stability in a physiological environment. These innovative technologies, combined with the development of shear-thinning bioinks with superior rheological properties, are driving extrusion-based bioprinting towards personalized, functional, and clinical applications[124](Fig 2. A).

2.2 Inkjet-based bioprinting

Inkjet-based 3D bioprinting achieves rapid layer-by-layer additive manufacturing by precisely controlling the ejection and deposition of microdroplets[125,126]. Its working principle is categorized into two main approaches: thermal inkjet technology uses heating elements to generate bubbles that push liquid bioink out of the printhead, with printhead temperatures typically ranging from 100-300°C, piezoelectric inkjet technology uses the mechanical deformation of piezoelectric ceramics to generate pressure pulses, ejecting droplets without heating, which is gentler on cells[127-129]. Inkjet technology is suitable for low-viscosity bio-inks, usually with viscosities between 1-30 mPa·s, commonly including: polysaccharide-based materials (sodium alginate, chitosan), protein-based materials (collagen, gelatin), synthetic polymers (PCL, PEG), and direct cell suspensions[130,131]. The primary limitations include relatively low

resolution, typically 100-200 μm, making microscopic structure design difficult; high-viscosity materials are prone to printhead clogging; and high temperatures and shear stress during thermal inkjet printing may affect cell viability (cell activity retention in thermal inkjet processes is usually 50-70%)[132]. However, its advantages are also prominent: fast printing speed (up to 1-10 cm^3/min) and low cost, especially piezoelectric inkjet printing, which does not require photoinitiators, thereby avoiding phototoxicity concerns.

In bone-tissue interface construction, inkjet technology can achieve precise organizational arrangement of multiple materials through the synchronous operation of multiple independent printheads, forming a gradient transition in mechanical properties; by combining synchronous ejection of calcium ions or other crosslinkers , different degrees of crosslinking and modulus changes can be achieved in different regions, seamlessly integrating hard bone regions (such as alginate incorporated with hydroxyapatite or tricalcium phosphate) with soft tissue regions. Its high efficiency is particularly suitable for constructing large-volume scaffolds.

Emerging derivative technologies of inkjet bioprinting are continuously expanding its application potential. Acoustic inkjet technology utilizes focused ultrasonic energy to drive liquid ejection, avoiding heating or pressure pulses, further further reducing cell damage while simultaneously improving inkjet precision[133,134]. Electro-jet technology drives conductive ~~bio-inks~~ bioinks by applying an electric field, enabling precise control of individual droplets, with resolution improved to 50-100 μm, making it particularly suitable for high-precision cell pattern printing. In-situ inkjet bioprinting integrates the inkjet system into surgical tools, allowing for real-time printing directly on a patient's wound or defect site, enhancing clinical operability. Furthermore, multi-axis inkjet systems, combined with robotic arms or six-axis motion platforms, enable the print head to move along complex three-dimensional paths, thereby transcending the limitations of planar layer-by-layer printing[135,136]. Biomarker inkjet allows for the simultaneous ejection of multiple colors or fluorescently labeled bio-inks, utilized for cell type differentiation and real-time tracking. The integration of these technologies is

driving inkjet printing towards higher precision, greater efficiency, and ~~closer clinical~~ more imminent clinical application[137].

2.3 Lithography-based bioprinting

Lithography-based 3D bioprinting utilizes photopolymerization to construct complex biological tissue scaffolds with high precision[138-140]. Its working principle involves irradiating bioinks containing photoinitiators with specific light (ultraviolet, visible, or near-infrared light). Technologies such as Digital Light Processing (DLP) or Stereolithography (SLA) project light patterns layer by layer or scan with lasers, photoinitiators in the bioink to undergo polymerization, thereby solidifying the liquid ink into the desired 3D structure[141,142]. This method is particularly suitable for hydrogel-based bioinks, such as Gelatin Methacryloyl (GelMA), Hyaluronic Acid Methacryloyl (HA-MA), and Polyethylene Glycol Diacrylate (PEGDA), which possess good biocompatibility and tunable mechanical properties, effectively encapsulating living cells[143,144]. Although photoinitiators and light exposure can be cytotoxic, the risk can be significantly reduced by selecting low-toxicity photoinitiators and utilizing gentler visible light or two-photon polymerization (2PP) techniques.

The advantage of this technology lies in its excellent resolution, with DLP achieving features in the tens of micrometers, and 2PP even reaching sub-micron (as low as approximately 100 nanometers) precision, coupled with fast printing speeds. This capability enables it to excel in constructing complex structures such as bone-tissue interfaces[145,146]. For example, by precisely controlling porosity, material gradients, and mechanical strength, hard bone regions (e.g., rigid hydrogels incorporating hydroxyapatite nanoparticles) can be seamlessly integrated with soft tissue regions (e.g., cell-rich elastic hydrogels), thereby replicating the biological and mechanical properties of natural interfaces and promoting effective inter-tissue integration[147,148].

Lithography-based bioprinting technology is continuously evolving, giving rise to various emerging derivative methods to overcome existing limitations and expand application boundaries. Notably, Tomographic volumetric additive manufacturing

(TVAM), also known as volumetric bioprinting, is a disruptive advancement. It no longer relies on layer-by-layer solidification but instead synchronously irradiates the entire bioink vat with dynamically adjusted light fields, forming a complete 3D structure in seconds to minutes[149-151]. This technique significantly increases printing speed, reduces shear stress on cells, and addresses the depth limitations of traditional layer-by-layer printing. 2PP is another cutting-edge technique that uses focused femtosecond pulsed near-infrared lasers to initiate polymerization exclusively at the focal point, achieving ultra-high resolution as low as 100 nanometers[152,153]. It is particularly well-suited for constructing microscopic scaffolds, cellular microenvironments, and delicate vascular or neural networks, while near-infrared light also minimizes cell damage. Furthermore, combining microfluidic technology for multi-material printing, high-throughput cell encapsulation, and developing portable lithography systems for in situ printing with handheld devices are current research hotspots. These emerging technologies, combined with next-generation bioinks and gentler photoinitiators, are collectively advancing bioprinting toward higher precision, faster speeds, and broader clinical applications (Fig 2. B) (Table 2).

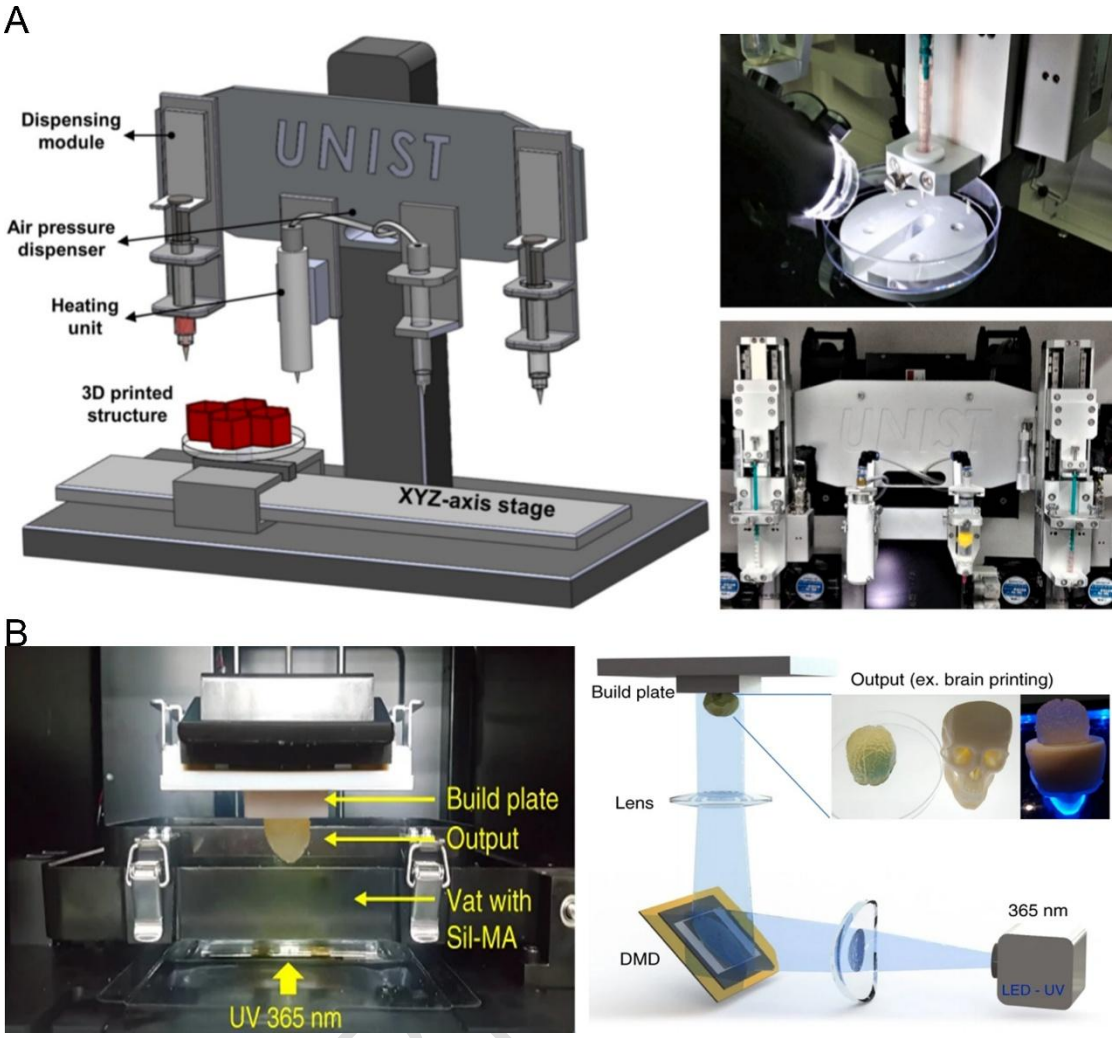

Figure 2. Schematic of 3D bioprinting methods. (A) A schematic diagram illustrates a 3D bioprinting system equipped with a three-axis motion platform and a multi-nozzle dispensing unit. The accompanying photograph presents the dispensing module fitted with four printheads, along with the fabrication process using dECM-based bioink. Reprinted with permission from Cui *et al.* [40]. Copyright © 2026, ELSEVIER. (B) LAP-functionalized Sil-MA was fabricated in a layer-by-layer manner using a digital light processing printer. Reprinted with permission from Wang *et al.* [154]. Copyright © 2026, Accscience Publishing.

Table 2. Comparative summary of extrusion-, inkjet-, and lithography-based bioprinting for bone–tissue interface regeneration

Parameter	Extrusion-based bioprinting	Inkjet-based bioprinting	Lithography-based bioprinting
Working principle	Pneumatic/piston/screw-driven extrusion of viscous bioink through a nozzle, deposited layer-by-layer	Thermal (bubble-induced) or piezoelectric (pressure-pulse) ejection of microdroplets	Photopolymerization by UV/visible/NIR light projection (DLP/SLA) or femtosecond laser (2PP)
Printing resolution	100–500 μm (nozzle/line width); MEW derivative reaches sub-micron (down to ~100 nm)	100–200 μm (thermal/piezoelectric); electro-jet improves to 50–100 μm	DLP: tens of μm; 2PP: down to ~100 nm (sub-micron)
Compatible bioink viscosity	Broad range; suited for highly viscous composite hydrogels (alginate, gelatin, collagen, HA, Pluronic, dECM)	Low viscosity only, typically 1–30 mPa·s (polysaccharides, proteins, PCL, PEG, cell suspensions)	Low–moderate viscosity; needs photocurable hydrogels (GelMA, HA-MA, PEGDA)
Achievable cell density	Up to 10^8 cells/mL	Relatively low; direct cell suspension printing possible	Moderate; high-throughput encapsulation achievable via microfluidics
Printing speed	Relatively slow	Fast, up to 1–10 cm^3/min	Fast (DLP/SLA); TVAM completes constructs in seconds–minutes
Cell viability	Often >90% after optimization	Thermal inkjet: 50–70%; piezoelectric gentler (higher viability)	High; phototoxicity minimized with low-toxicity initiators/visible light/2PP
Major advantages	Region-specific deposition of multiple materials (hard bone + soft tissue); high cell density; good mechanical strength and dimensional stability; handles diverse viscous bioinks	Fast speed and low cost; no photoinitiator needed (piezoelectric) avoiding phototoxicity; multi-head synchronous printing for gradients	Excellent resolution and fast speed; precise continuous gradients in mineral/stiffness at micro-scale; ideal for vascular/neural-scale structures

Limitations	Relatively low resolution; slow speed; shear-stress damage to cells	Low resolution; high-viscosity inks clog printhead; thermal heating (100–300 °C) reduces viability	Photoinitiator and light exposure can be cytotoxic; depth limits in layer-by-layer printing
Suitability for bone–tissue interfaces	Best for co-depositing bone-phase (HAp ceramics) + soft-tissue (cell-rich hydrogels) in regionalized gradients; ideal for bone-cartilage/bone-tendon	Efficient for large-volume scaffolds and gradient crosslinking via synchronous multi-head; suitable for bone-cartilage and bone-vessel	Best for constructing micro-scale continuous gradients (mineral/stiffness); excellent for precise vascular/neural microstructures and complex interface geometries

Abbreviations: 2PP: Two-photon polymerization; DLP: Digital light processing; dECM: Decellularized extracellular matrix; GelMA: Gelatin methacryloyl; HA: Hyaluronic acid; HA-MA: Hyaluronic acid methacryloyl; HAp: Hydroxyapatite; MEW: Melt electrowriting; mPa·s: Millipascal-second; NIR: Near-infrared; PCL: Polycaprolactone; PCR: Polyethylene glycol; PEGDA: Polyethylene glycol diacrylate; PEG: Polyethylene glycol; SLA: Stereolithography; TVAM: Time-varying absorption modulation; UV: Ultraviolet.

3. 3D Bioprinting to Repair Bone-Tissue Interfaces

3.1 Bone and cartilage

The application of 3D bioprinting in osteochondral interface repair began with mimicking the hierarchical structure of native tissues. Early studies achieved spatial separation of cartilage and bone layers through simple biphasic constructs, utilizing different hydrogel systems (such as alginate-gelatin mixtures) and ceramic fillers (such as hydroxyapatite) to support cartilage matrix and bone formation, respectively[59]. However, the key breakthrough was recognizing the unique biological function of the interface itself, it must simultaneously block vascular invasion (thereby preventing inappropriate endochondral ossification), maintain mechanical gradient transitions, and facilitate signal communication between adjacent tissues. This propelled researchers from passive structural design to active interface engineering, such as physically preventing vascular ingrowth through precise pore size control (< 6 μm)[30], or achieving enhanced adhesion strength (> 6.5 times) through embedded designs of fiber-reinforced networks[54].

The regulation of cell differentiation has evolved from single chemical inducing factors to multi-dimensional physical-metabolic coupling strategies. Traditional methods relied on spatially stratified nutrient gradients or cytokine diffusion, exhibiting limited efficiency[53]. Current innovations include: inhibiting cartilage hypertrophy and promoting stable hyaline cartilage phenotype maintenance through hypoxic microenvironments; leveraging microRNAs to directionally program the osteogenic or chondrogenic differentiation potential of stem cells in specific regions[57](Fig 3. E), and integrating mechanical stiffness gradients with metabolic activity gradients, allowing bone marrow-derived stem cells to form cartilage in soft and hypoxic regions and bone in hard and vascular-rich regions[64]The most cutting-edge strategies even introduce piezoelectric nanozymes responsive to ultrasound stimulation, achieving coupled regulation of mechanoelectric signals and reactive oxygen species scavenging on the same platform[63](Fig 3. A-D).

The development of bioprinting technology itself has advanced the feasibility of

osteochondral interface engineering. Integrated printing systems with multiple axes, processes, and materials (combining extrusion, electrospinning, and digital light processing) have made it possible to simultaneously obtain different mechanical gradients, pore structures, and cell densities in a single manufacturing run[30]. The introduction of scaffold-free bioprinting has further streamlined the manufacturing process—by precisely positioning and in situ fusing pre-differentiated heterotypic cell spheroids, histologically relevant interface structures are directly constructed, avoiding stress transition mismatch during long-term scaffold degradation[55]. DLP high-resolution printing enables precise programming of gradient interfaces, allowing for continuous transitions in mineral phase content and stiffness at the micro-scale, compatible with in situ crosslinking and high cell viability[62].

3D bioprinted osteochondral interfaces have demonstrated significant repair efficacy in large animal models (goats) and rat defect models. Biphasic fiber-reinforced cartilage templates achieved more hyaline-like cartilage regeneration in 6-month goat intra-articular cartilage defect repair[56], while DLP-printed collagen-based gradient scaffolds achieved near-complete recovery of cartilage and bone within 12 weeks[62]. More significantly, these materials are being endowed with additional functional dimensions—immunomodulatory functions (achieving sequential pro-inflammatory to anti-inflammatory conversion through the coupling of natural biomaterials and metal-organic frameworks)[61], marking a shift from passive replacement to active treatment. Simultaneously, these constructs have begun to serve as physiologically relevant platforms for in situ disease modeling and drug screening[64], providing new possibilities for preclinical evaluation and personalized medicine.

Comparatively, osteochondral bioprinting has progressed through three distinct design logics. Pore-size regulation and fiber-reinforced architectures mainly address structural biomimicry and interface stability, because they improve mechanical continuity, strengthen hydrogel–ceramic bonding, and help reproduce the layered organization of cartilage and subchondral bone. In contrast, hypoxic microenvironments, microRNA programming, and mechanical–metabolic dual

gradients are more biological instruction strategies, with their primary aim being to steer region-specific stem-cell differentiation and preserve a stable chondrogenic phenotype. Piezoelectric nanozyme-based systems represent a more advanced but also more complex approach, as they couple mechanotransduction with reactive oxygen species regulation and therefore extend beyond passive structure matching toward active microenvironment control.

In terms of validation, fiber-reinforced and gradient scaffolds have shown the strongest in vivo evidence, including repair in rabbit, rat, and goat models; by comparison, spheroid-based and miRNA-engineered constructs are often more mature as in vitro or proof-of-concept platforms, although they provide valuable mechanistic insight. Overall, structural reinforcement is better suited for defects requiring immediate load-bearing and interfacial integrity, whereas hypoxia-, gene-, and signal-responsive strategies are more appropriate when the goal is to direct cell fate and improve long-term biological maturation. The main unresolved issue is how to synchronize these functions temporally, since cartilage maintenance, subchondral bone formation, and vascular exclusion do not occur on the same timescale.

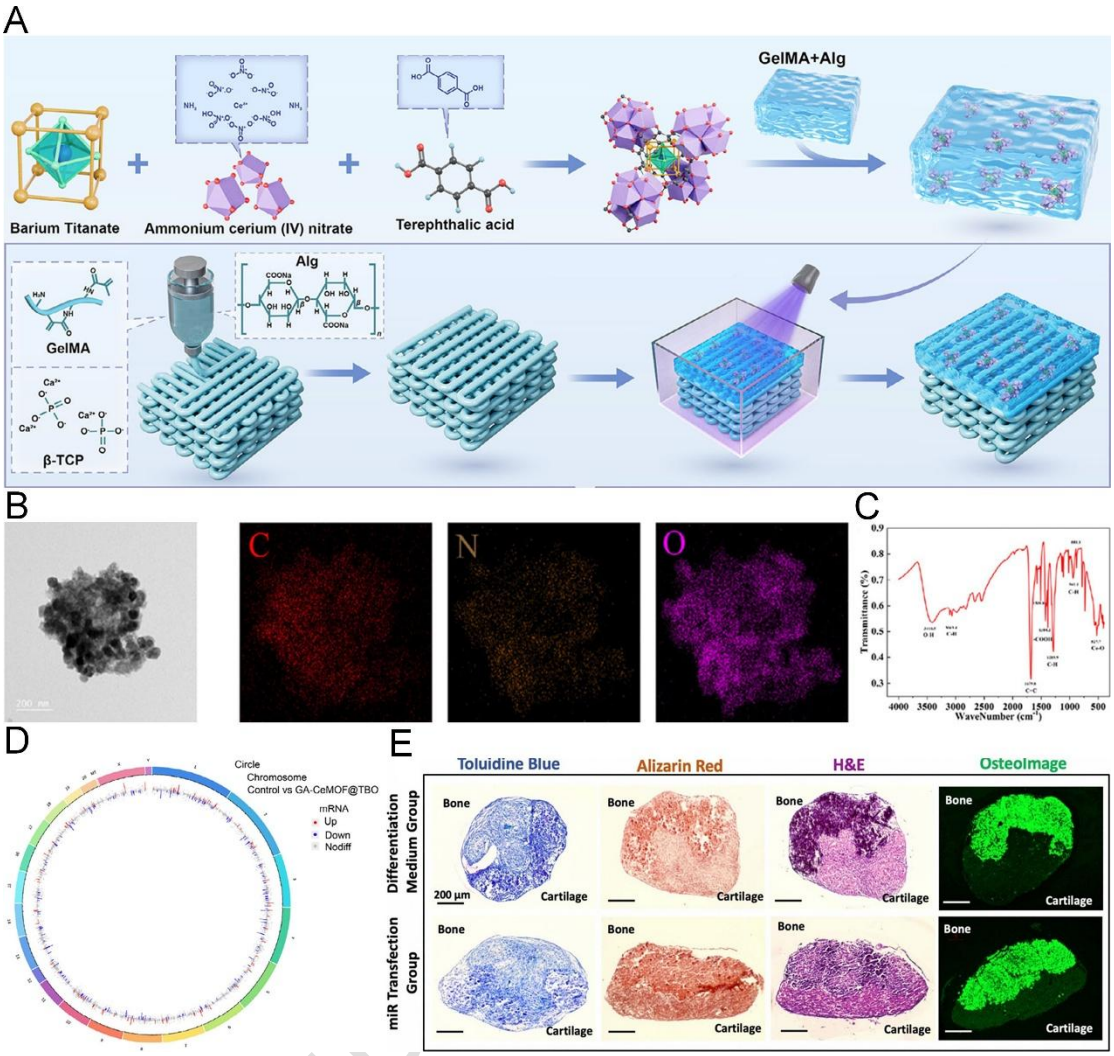

Figure 3. 3D bioprinting for bone-cartilage interface regeneration. A. A biphasic osteochondral interface repair scaffold was designed and prepared using 3D printing technology. The upper layer is GC-CeMOF@BTO for cartilage repair, and the lower layer is GB-tricalcium phosphate for bone repair. B. TEM morphology image of CeMOF@BTO(Left). STEM/EDS elemental mapping images of CeMOF@BTO (right). C. Fourier-transform infrared (FTIR) spectrum of CeMOF@BTO. D. Transcriptome analysis and functional enrichment of differentially expressed genes after GC-CeMOF@BTO treatment: circular genomic map. Reprinted with permission from Ding *et al.*[63]. Copyright © 2026, WILEY-V C H VERLAG GMBH. E. Histochemical staining of the bioprinted osteochondral interfaces for (a) Toluidine Blue, Alizarin Red, H&E, and OsteoImage. Reprinted with permission from Celik et al.[57]. Copyrighr © 2022, IOP Publishing Ltd.

3.2 Bone and blood vessels

The repair of large bone defects presents significant challenges in the field of tissue engineering, with the core issue being the absence of an effective vascular network to supply oxygen and nutrients and remove metabolic waste, leading to central cellular

necrosis and impaired tissue function. 3D bioprinting, as a technology capable of precisely controlling the spatial arrangement of cells and materials, offers unique advantages for constructing functional vascularized bone tissue. Early research primarily focused on co-culturing osteoblasts (such as human bone marrow mesenchymal stem cells, hMSCs, or adipose-derived stem cells, ASCs) and vascular endothelial cells (such as human umbilical vein endothelial cells, HUVECs) to simulate the angiogenesis and osteogenesis processes of bone[66,69,155]. By loading these cells into printable hydrogel bioinks (such as GelMA, fibrin) and designing scaffold structures containing interconnected microchannels, preliminary achievements included the in vitro growth, migration, and organization of vascular cells, as well as the proliferation and osteogenic differentiation of bone cells, thereby establishing a foundation for constructing perfusable tissues[65].

Inspired by natural osteons (concentric circular structures composed of blood vessels and layers of osteocytes in compact bone), numerous studies have focused on three-dimensional printing of scaffolds with osteon-mimicking structures. By precisely constructing hierarchical microchannels such as vertical central medullary canals, Haversian canals, and Volkmann's canals, these scaffolds guide the distribution of vascular endothelial cells and the formation of vascular networks, thereby enhancing in vivo vascularization capacity[68,72]. Simultaneously, the optimization and functionalization of bioinks have become crucial. By incorporating bioactive ceramic materials such as nanohydroxyapatite (nHA), silicate nanoplatelets, or polydopamine-modified calcium silicate (PDACS), not only are the mechanical strength and osteoinductive capabilities of the scaffolds enhanced, but also the growth of vascular endothelial cells and the development of vascular networks are promoted[67,70]. Additionally, the introduction of bioactive molecules such as vascular endothelial growth factor (VEGF) or CD34+ cell enhancing factors (e.g., SR1 nanoparticles) can specifically promote angiogenesis, further improving the regenerative potential of vascularized bone tissue[28,66].

To achieve the construction of larger and more complex vascularized bone tissues,

3D bioprinting technology itself is continuously innovating. Dual-ink and coaxial 3D bioprinting technologies enable precise spatial separation of bioinks, encapsulating osteoblasts and vascular endothelial cells in different regions of the scaffold, creating a non-contact co-culture environment that optimizes intercellular signal communication, and thus more effectively promoting angiogenesis and bone formation[70,73](Fig 4. E). In addition, the in vitro pre-vascularization strategy is widely explored, where stable microvascular networks are induced to form in constructs during the in vitro culture phase before being implanted in vivo. Studies have shown that fibrin-based bioink constructs containing only HUVECs and supportive hBMSCs, when matured in vitro and subsequently implanted into critical-sized bone defect models, significantly increase vascularization levels and promote new bone formation[71] . Recently, research has proposed modular living assembled bone organoids, combined with in situ guided vascularization strategies, to achieve high-throughput modular bone organoid assembly through bioprinting and induce the formation of tubular structures with unidirectional guided vascularization. This approach offers possibilities for one-step surgical transplantation and rapid perfusion, potentially advancing vascularized bone tissue towards clinical translation[75](Fig 4. A-D). Some studies have even begun to explore bioprinting inorganic biomaterials with neural stem cells, promoting the synergistic regeneration and functional recovery of multiple tissues, including bone, blood vessels, and even nerves, from a neuro-inductive perspective[74] , which indicates the increasingly heightened complexity anticipated in future tissue engineering endeavors.

Among vascularized bone strategies, the main distinction lies between architectures that create space for perfusion and systems that actively induce vessel maturation.

Osteon-mimetic microchannels, interconnected pores, and scaffold architectures with predefined lumens primarily improve structural transport efficiency by enabling nutrient diffusion and guiding endothelial invasion. These designs are especially valuable in thick constructs or large defects, where mass transport is the first limiting factor. By contrast, cell co-culture systems, VEGF or SR1 delivery, and

prevascularization strategies focus more on biological activation, aiming to accelerate endothelial network formation and improve the coupling between angiogenesis and osteogenesis.

In experimental terms, simple channel-based and osteon-like scaffolds have already shown robust in vivo relevance, whereas modular organoid assembly and more elaborate guided vascularization systems remain comparatively early-stage, despite their translational promise. The advantage of prevascularized constructs is that they can shorten the host-implant lag phase after implantation, but their limitation is the difficulty of maintaining lumen stability and perfusion after scaling up. Therefore, channel design is best used when the priority is rapid oxygen delivery and construct survival, whereas growth-factor- or cell-driven approaches are more suitable when mature vasculature and long-term osteogenesis are required. A central challenge remains the establishment of vessels that are not only present, but also stable, perfusable, and functionally integrated with bone remodeling.

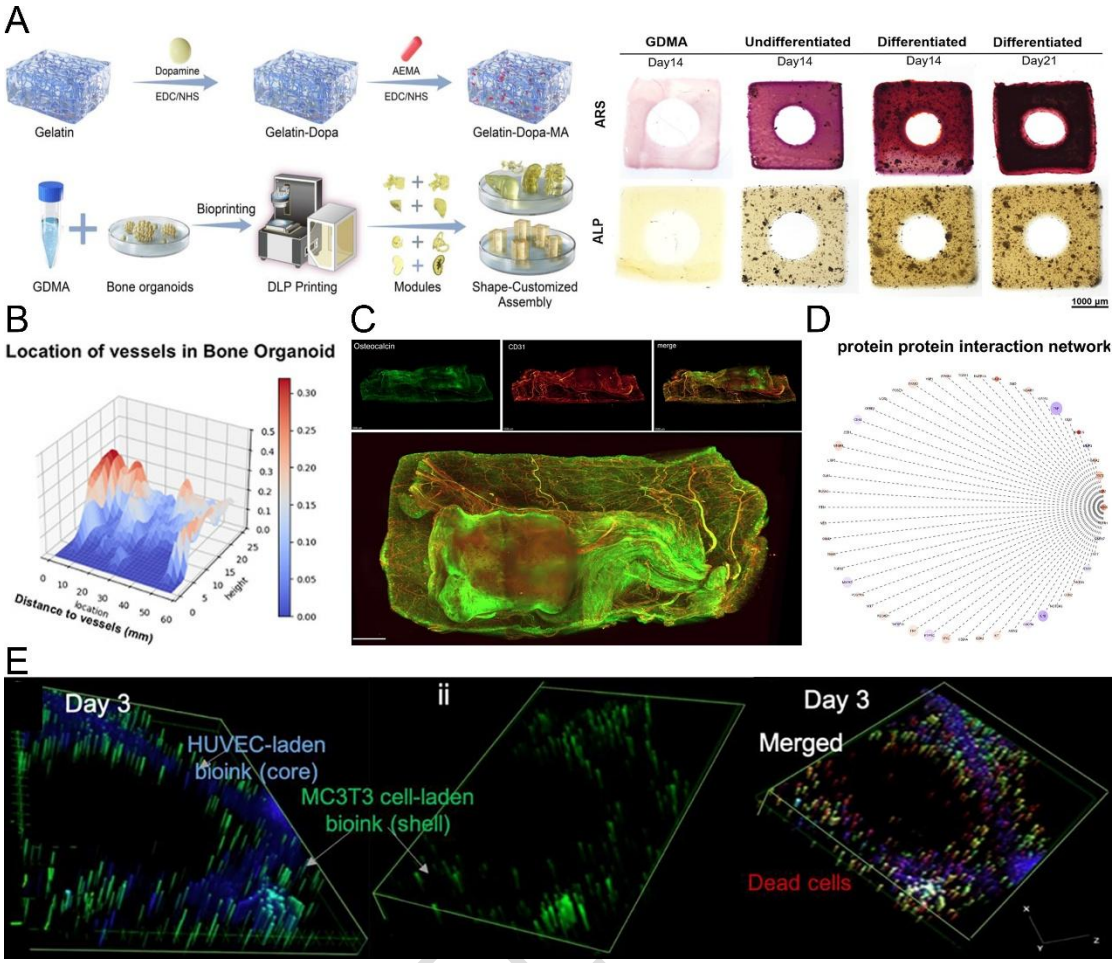

Figure 4. 3D bioprinting for bone-vascular interface regeneration. A. The synthesis of hydrogels and the modular printing, assembly and vascularization process of bone organoids (left). GDMA hydrogel for the induction and culture of bone organoids. Alizarin Red S (ARS) and alkaline phosphatase (ALP) staining of printed bone organoid modules following in vitro osteogenic induction (right). B. Evaluation of bone organ maturation and vascularization after implantation (2,4,8,12 weeks): Fluorescence intensity analysis and three-dimensional spatial quantification were performed on the cleared samples. C. The overall transparency of the bone tissue-skin composite material, the double immunofluorescence of CD31 / OCN, and the 3D imaging under the light sheet microscope. D. A protein-protein interaction network centered on Sox9. Reprinted with permission from Ju et al.[75]. Copyright © 2026, KEAI PUBLISHING LTD. E. The visualization and cell distribution of bioprinted structures under confocal microscopy, Representative 3D volume viewer of the core-shell structure on day 3 of culture. Reprinted with permission from Shahabipour et al.[73]. Copyright © 2022, WILEY.

3.3 Bone and nerves

3D bioprinting technology, with its unique spatial precision control capabilities, provides an unprecedented tool for constructing complex microenvironments that support both bone and nerve regeneration. It enables the precise positioning of nerve

cells and bone-related cells and simulates the simplified spatial distribution found in natural bone, thereby achieving intraosseous nerve regeneration. Early research has demonstrated that photocrosslinkable and biodegradable polymers such as OPF can serve as bioinks, supporting the good survival and proliferation of osteocytes and nerve cells, laying a material foundation for bone-nerve regeneration[76].

To effectively promote bone-nerve interface repair, research focus has shifted from the application of single cells or materials to the synergy of multi-dimensional bioactive factors and cellular strategies. By integrating nerve growth factor (NGF) into bioprinted structures, the microenvironment of the osteogenic center can be simulated, promoting axonal extension and inducing sensory neurons to secrete calcitonin gene-related peptide (CGRP), which in turn stimulates osteogenic differentiation and inhibits adipogenesis, ultimately improving bone regeneration in cranial defect models[77]. Similarly, Schwann cells promote the proliferation and differentiation of bone marrow mesenchymal stem cells and the migration and tubule formation of endothelial progenitor cells through the secretion of exosomes (SC-exos), thereby mimicking Schwann cell-mediated neuro-osseous crosstalk, optimizing the bone repair microenvironment, and promoting the synergistic regeneration of nerves, blood vessels, and bone[81]. In addition, inorganic biomaterials also play a crucial role. For example, calcium silicate nanowires (CS nanowires) integrated into bioinks act as "bioactive factors" significantly promoting the long-term survival, spreading, and osteogenic and neurogenic differentiation of encapsulated cells, thereby accelerating new bone formation and nerve fiber ingrowth[79]. Some studies have even utilized bioprinted scaffolds to deliver neuromodulators, such as inhibiting sympathetic activation and catecholamine release through sustained-release calcium channel blocker nifedipine to promote bone defect repair[80], and enhancing bone regeneration through the synergistic effect of CGRP and β-adrenergic receptor antagonist propranolol (PRN)[82](Fig 5. D). These strategies collectively emphasize the profound understanding of neuro-osseous interactions and the importance of multi-signal biological regulation.

With the continuous development of 3D bioprinting technology, researchers are

able to construct increasingly complex and functional bone-nerve interface structures. Multi-cell 3D bioprinting technology enables the layered printing of nerve cells (such as Schwann cells RSC96) and bone marrow mesenchymal stem cells, and functionalizes the neurogenic and osteogenic layers with covalently linked NGF and BMP-2 mimetic peptides, thereby promoting the long-term survival and differentiation of both cell types in spatially heterogeneous constructs, and achieving synergistic enhancement of neurogenesis and osteogenesis both in vitro and in vivo[84]. To address peripheral nerve injury, multi-nozzle pressurized 3D bioprinting technology has been used to fabricate bilayer nerve conduits. The combination of GelMA encapsulating BMSCs in the inner layer and high mechanical strength GelMA/PEGDA in the outer layer not only supports high cell viability and extensive cell spreading but also effectively promotes the adhesion and proliferation of PC12 nerve cells[78]. More forward-looking research has explored the combination of bio-inspired piezoelectric bioprinted scaffolds with neurons, utilizing piezoelectric polylactic acid (PLLA) to mediate mechano-electrical coupling under ultrasound stimulation, triggering Ca^{2+} influx within integrated dorsal root ganglion (DRG) neurons, thereby enhancing CGRP secretion, further promoting osteogenesis and angiogenesis, and accelerating neurovascularized bone regeneration. This represents a new strategy for constructing functional interfaces with sensing-effect self-consistent circuits[85](Fig 5. A-C). These advancements indicate the immense potential of 3D bioprinting in achieving highly integrated regeneration of nerves, blood vessels, and bone in complex tissues, laying the foundation for the future development of vascularized innervated scaffolds[74,83].

Compared with vascularized bone constructs, bone–nerve strategies place greater emphasis on bioelectrical signaling and neuro-osteogenic crosstalk rather than on perfusion alone. Bioink formulations containing NGF, Schwann cells, neural stem cells, or conductive/piezoelectric components mainly serve to promote innervation and modulate osteogenesis indirectly through neurotrophic and mechanoelectrical pathways. These designs are particularly effective when the therapeutic goal is to restore sensory or sympathetic regulation, or to reproduce the neurovascular niche that

supports bone healing. In contrast, scaffold designs with bilayer conduits or aligned architectures are more focused on structural guidance and nerve regeneration, and therefore are closer to peripheral nerve engineering than to fully integrated bone repair.

The validation level also differs substantially among the reported approaches. Simple cell-supportive biinks and bilayer conduits have clear in vitro and small-animal validation, while systems that use Schwann cell exosomes, neurotransmitter modulation, or piezoelectric interoception circuits are conceptually more advanced but remain less extensively tested. In practical terms, the field is moving from “nerve-compatible bone scaffolds” toward “neuroactive regenerative scaffolds,” yet most studies still stop short of demonstrating durable functional restoration in large defects. Thus, the most realistic near-term application is in defects where impaired innervation contributes to delayed healing, while full sensory-motor reconstruction remains a longer-term goal.

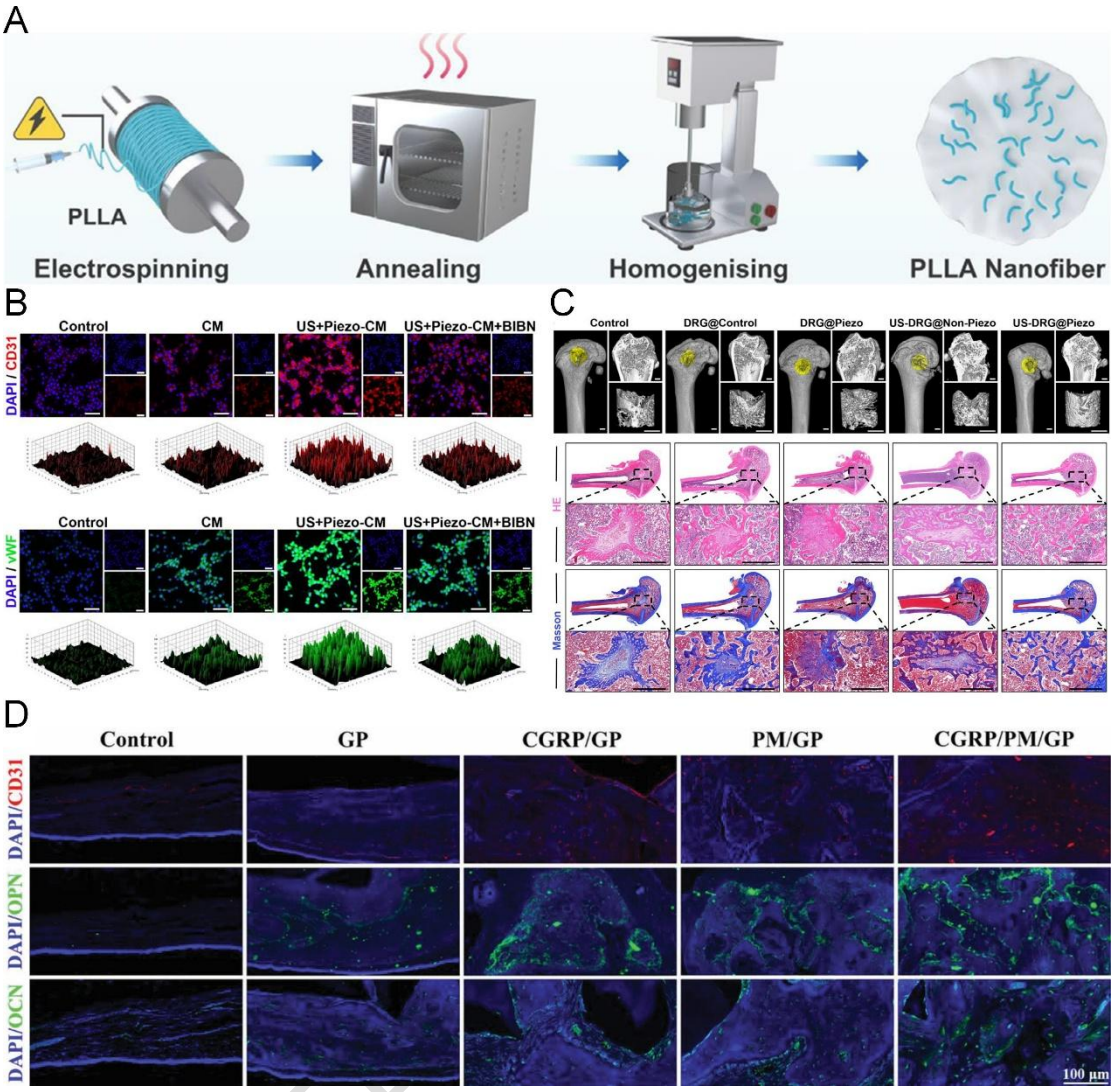

Figure 5. 3D bioprinting for bone-nerve interface regeneration. A. A schematic diagram of the preparation of piezoelectric polylactic acid nanofibers.B. If the micrographs show CD31 (red) in different groups of endothelial progenitor cells, the nucleus (up) is counterstained with DAPI (blue). If vWF (green) micrographs were depicted in different groups of EPCs, the nuclei (down) were counterstained with DAPI (blue). C. The bone regeneration effect of neurobioimprinted piezoelectric scaffold in vivo for 4 weeks. Micro-CT images, H & E and Masson staining images of bone defect areas in different groups: control group, DRG @ Control, DRG @ Piezo, US-DRG @ Non-Piezo, US-DRG @ Piezo. Reprinted with permission from Su et al.[85]. Copyright © 2026, WILEY-V C H VERLAG GMBH. D. Immunofluorescence staining was used to evaluate the fluorescence images of CD31 (red), OCN (green) and OPN (green) at 10 weeks after stent implantation. The nuclei were stained with DAPI (blue). Reprinted with permission from Guo et al.[82]. Copyright © 2023, WILEY-V C H VERLAG GMBH.

3.4 Bone and tendons

The osteotendinous interface (enthesis) is a highly complex gradient tissue, whose primary function is to smoothly transfer mechanical loads from soft tissue (tendon) to

hard tissue (bone), thereby preventing stress concentration. However, when a tendon tear occurs (such as a rotator cuff tear or anterior cruciate ligament reconstruction), this interface typically forms fibrous scar tissue rather than regenerating a normal attachment point with a mechanical gradient, leading to poor repair outcomes and high re-tear rates. 3D bioprinting technology offers a new solution for this, as it can precisely control the spatial arrangement of cells and materials, with the goal of reconstructing this natural gradient structure. Early research focused on using bioprinted scaffolds loaded with mesenchymal stem cells to enhance osteointegration between the tendon and bone tunnel, for example, in a rabbit model of anterior cruciate ligament reconstruction, 3D bioprinted scaffold sleeves with MSCs significantly promoted osteointegration and fibrocartilage formation[86] . Additionally, research has explored printing recombinant spider silk hydrogels with fluorapatite composite materials to generate biomaterial structures with mechanical gradient properties, mimicking the mechanical transition characteristics of natural attachment points[88] . Multicellular bioprinting strategies have further been employed to develop biomimetic inks, combining tendon/bone-related cells and Mo-silicate bioceramics, to simulate the hierarchical structure and cellular composition of the interface, thereby achieving synchronous multi-tissue repair[91].

To more effectively promote the regeneration of the osteotendinous interface, merely mimicking the structure is not enough; precise regulation of cell differentiation and tissue formation is equally essential. Current strategies emphasize the introduction of various bioactive factors and functional materials to guide the directed differentiation of stem cells into tenocytes, chondrocytes, and osteoblasts into spatially distinct regions. Among these, spatiotemporally precise delivery of growth factors is a key pathway. For example, by embedding microspheres loaded with tenogenic, chondrogenic, and osteogenic growth factors in 3D printed scaffolds, sustained and spatially controlled release of GFs can be achieved, thereby guiding the differentiation of mesenchymal progenitor cells in vitro to form multiphasic tissues with tendon-like, cartilage-like, and bone-like regions, and promoting the formation of fibrocartilaginous interfaces and

integrated healing in vivo by recruiting endogenous tendon progenitor cells[87](Fig 6. B, C). Furthermore, this layer-specific growth factor loading strategy has been applied to construct living tissues, substantially enhancing attachment point regeneration in rotator cuff tear models, including improved biomechanical properties, collagen deposition, and alignment[89] (Fig 6. A, B, E), by guiding the in situ differentiation of loaded stem cells. Additionally, research has further enhanced the ability to induce cell differentiation by coating specific dECM onto 3D printed gradient biomimetic scaffolds (GBS), achieving tendon-bone differentiation characteristics similar to natural attachment points and significantly improving biomechanical properties[90].

With advancements in bioprinting technology, researchers are able to construct increasingly complex gradient tissues that more closely approximate natural attachment point structures. For example, using a coaxial nozzle system for 3D bioprinting can effectively and synchronously fabricate aligned tendon tissue, a gradient tendon-bone interface (TBI), and mechanically enhanced bone regions, thereby mimicking the natural tendon-bone structure. This method not only improves mechanical properties and tissue integration but also promotes angiogenesis and extracellular matrix formation, demonstrating the potential for rapid regeneration of full-layer tendon-bone tissue in rabbit rotator cuff tear models[92] . Similarly, by using a core-shell nozzle-assisted bioprinter, combined with collagen microbeads loaded with bone morphogenetic protein 2 (BMP-2), a multilayer scaffold was constructed, achieving a gradient decrease in BMP-2 content from the bone to the tendon region, accelerating the remodeling of full-layer osteotendinous tissue in rabbit rotator cuff tear models[93] . These advanced bioprinting strategies, integrating sophisticated designs of materials, cells, and bioactive molecules, have achieved encouraging preclinical results in animal models, indicating the immense clinical translational potential of 3D bioprinting in future clinical treatment of osteotendinous interface injuries, improving surgical success rates and enhancing the quality of patient recovery.

Tendon-to-bone bioprinting is distinguished by its focus on load transfer and enthesis remodeling, which makes mechanical matching more critical here than in most

other bone-interface systems. Scaffolds based on MSC loading or endogenous progenitor recruitment mainly improve cellular participation and interface healing capacity, but their structural mimicry is often relatively simple. By contrast, gradient printing, coaxial or core-shell systems, and dECM-coated constructs are designed to reproduce the native transition from tendon to fibrocartilage to bone, and therefore are better suited to structural and compositional biomimicry. Layer-specific growth factor delivery adds another level of control by directing region-specific differentiation, but it does not fully solve the problem of matching the evolving mechanical environment during healing.

Compared with osteochondral and vascularized bone studies, tendon-to-bone research has more clearly demonstrated functional improvement in animal models, including enhanced histology, collagen alignment, fibrocartilage formation, and biomechanical outcomes. However, the field still faces a major limitation: the degradation of the printed construct and the maturation of regenerated tissue are often not synchronized, which can compromise long-term repair. Therefore, simple MSC-seeded sleeves may be suitable for proof-of-concept or adjunctive repair, whereas graded, growth factor–patterned, and dECM-guided systems are more relevant for true enthesis reconstruction in load-bearing settings.

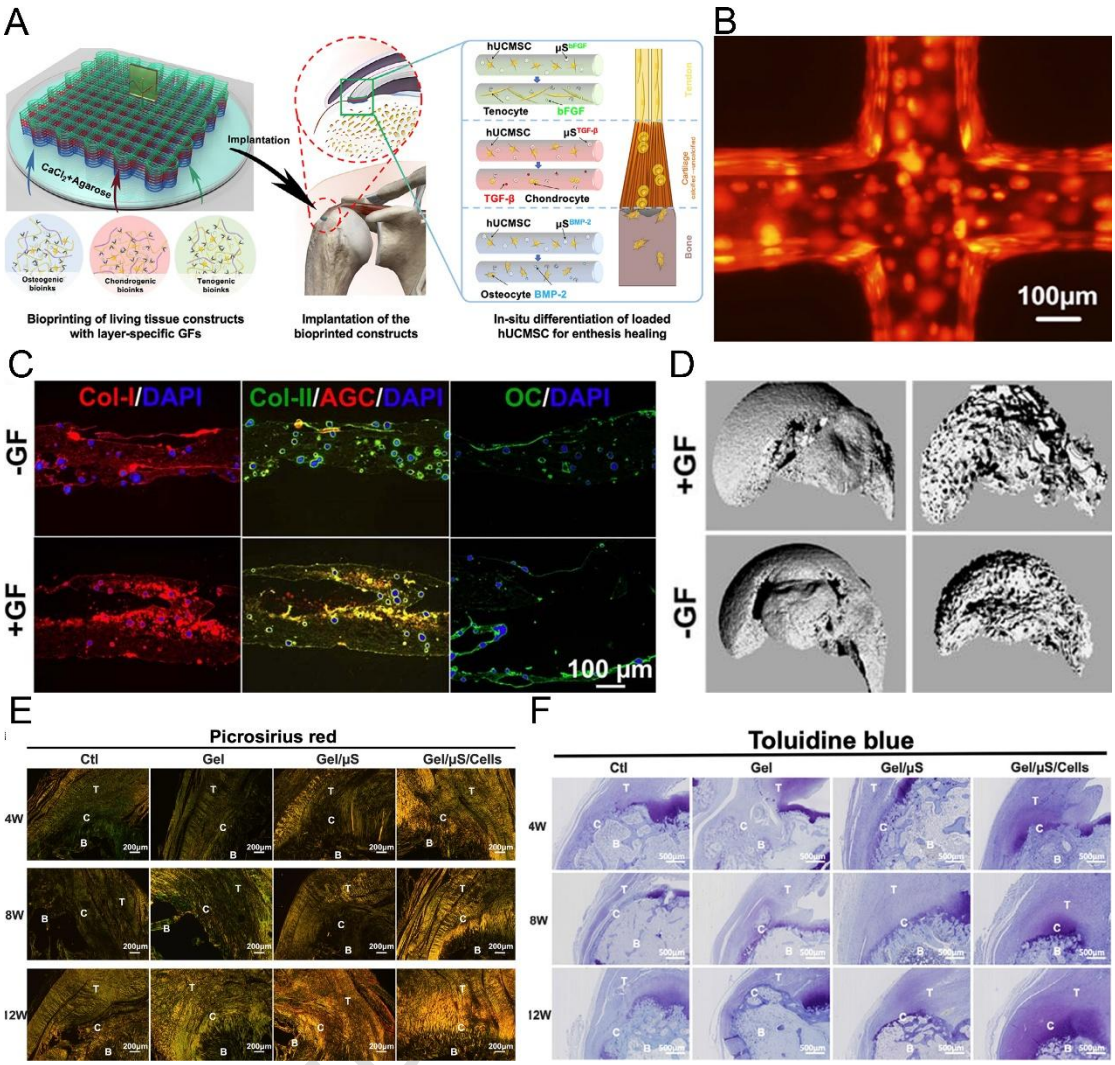

Figure 6. 3D bioprinting for bone-vascular and bone-tendon interface regeneration A. Implantation of bioprinted living tissue constructs a layer-specific GFs-loaded μS to promote banded tendon formation, cartilage formation, and osteogenesis during rotator cuff healing. B. Fluorescent images of bioprinted cell carriers. Reprinted with permission from Bai et al.[89]. Copyright © 2022, ELSEVIER SCI LTD. C. The rotating scaffold implanted in the space-time delivery system can guide human bone marrow mesenchymal stem cells to differentiate into fibrocartilage matrix gradient tissues with high tensile modulus. D. Micro-CT images of three-dimensional reconstruction showed bone loss in the cortex and trabecular bone of the humeral head due to supraspinatus tendon-to-bone repair treatment. Reprinted with permission from Tarafder et al.[87]. Copyright © 2020, IOP Publishing Ltd. E. Collagen and cartilage regeneration of the retrieved terminal tissue: typical impression red staining images of depressions retrieved at 4,8 and 12 weeks after surgery. F. Toluidine blue staining images taken at 4,8 and 12 weeks after surgery. Reprinted with permission from Bai et al.[89]. Copyright © 2022, ELSEVIER SCI LTD.

3.5 Bone and immunity

Not all studies discussed in this section involve direct cell-laden bioprinting;

several are conventional 3D-printed scaffold studies. They are included here because scaffold architecture, pore geometry, and material composition are upstream determinants of osteoimmune regulation and therefore remain directly relevant to the review's central theme of interface-oriented biofabrication.

Bone tissue repair is a complex process, in which the host's immune response to implanted materials is crucial for the outcome of bone regeneration. Traditional bone repair strategies often overlook the critical importance of the immune microenvironment in the early stages of fracture healing. 3D bioprinting technology, through its precise control over the spatial arrangement of cells and materials, provides a unique tool for actively modulating the bone-immune interface. Early research and strategic insights recognize that dual-channel co-encapsulation bioprinting of bone marrow-derived macrophages (BMMs) and bone marrow mesenchymal stem cells can leverage paracrine effects between cells to promote M2-type (anti-inflammatory, pro-repair) polarization of macrophages in the early stages of bone defects, reducing excessive inflammatory responses and thus creating favorable conditions for subsequent bone formation, ultimately accelerating bone repair[50]. Beyond cellular-level regulation, the physical properties of biomaterials have also been shown to significantly affect the immune response. Studies have found that the pore size of 3D printed scaffolds plays a decisive role in macrophage polarization and foreign body reaction (FBR). For example, polycaprolactone/polyethylene glycol/hydroxyapatite (PCL/PEG/HA) scaffolds with larger pore sizes (e.g., P600 scaffolds with 582.1 ± 27.2 μm) can significantly reduce foreign body reactions, promote enhanced M2-type macrophage infiltration, blood vessel ingrowth, and new bone formation, revealing the direct regulatory role of scaffold physical structure on the immune response during bone regeneration[94] (Fig 7. D-E).

To achieve more precise and efficient repair of the bone-immune interface, 3D bioprinting strategies have further advanced to actively induce immune cell behavior through functionalized biomaterials and to mechanistically their molecular mechanisms. For example, by chemically modifying Apt19s (an aptamer that specifically recruits

BMSCs) onto the surface of 3D printed GelMA/Laponite hydrogel scaffolds, it not only significantly enhances the recruitment and adhesion of BMSCs but also induces macrophages to undergo polarization from M1 to M2 type. Further RNA sequencing analysis revealed that macrophages promote osteogenic differentiation of BMSCs by regulating the AMPK/mTOR signaling pathway, providing a profound mechanistic understanding for enhancing bone repair through the osteoimmune pathway[95]. Furthermore, integrating metal-organic framework (MOF) nanoparticles (such as luteolin-loaded ZIF-8) into 3D bioprinted GelMA hydrogel scaffolds can achieve sustained release of bioactive components (luteolin and zinc ions), thereby endowing the scaffolds with multiple functionalities including antibacterial, osteoinductive, and inflammation-modulating properties. Such functionalized scaffolds can regulate the immune microenvironment, promote osteogenic differentiation of BMSCs, and have demonstrated their osteoimmune regulation and osteogenic capabilities in in vivo experiments[96]. Collectively, these studies underscore that 3D bioprinting, through ingenious material design and functionalization, can not only regulate immune responses at the bone-immune interface but also transform them into catalytic forces promoting bone regeneration, thereby achieving more efficient and targeted bone tissue engineering strategies.

Bone-immune interface studies differ from the other sections because their primary target is not tissue replacement itself, but the regulation of host response that determines whether repair can proceed successfully. Compared with osteochondral, vascular, or tendon-to-bone constructs, these systems are less focused on reproducing a specific anatomical gradient and more focused on controlling macrophage behavior, foreign body response, and the timing of inflammatory resolution. Pore-size regulation is the most direct structural approach and has the advantage of being simple, scalable, and compatible with conventional scaffolds, but it is relatively coarse in biological specificity. By contrast, aptamer functionalization and MOF-based ion/drug delivery provide more precise immunomodulation and can simultaneously recruit stem cells or enhance osteogenesis, yet they are more chemically complex and still require careful

safety evaluation.

In terms of validation, pore-architecture studies and functionalized hydrogel scaffolds have already shown convincing in vivo anti-inflammatory and osteogenic effects, but the field remains early in defining reproducible rules for timing, dose, and immune-state transitions. The strongest contribution of this section is therefore mechanistic: it shows that interface repair depends not only on biomimetic structure, but also on converting early immune responses into pro-regenerative signals. The best application scenario is in defects with high inflammatory burden, implant-associated irritation, or poor healing propensity, where immune modulation may be more decisive than simply adding more osteogenic cues.

3.6 Bone and ligaments

The osteoligamentous enthesis, a critical junction where tendons or ligaments connect to bone, possesses a unique gradient structure, composition, and mechanical properties, making it exceptionally challenging for functional tissue to regenerate spontaneously after injury. 3D bioprinting technology, with its precise control over the spatial arrangement of cells and materials, offers unprecedented opportunities for constructing and repairing this complex interface. On one hand, 3D bioprinting is employed to create highly biomimetic in vitro microtissue models to deeply investigate the biological mechanisms and pathological processes of the interface. For example, researchers have successfully constructed a multicellular periodontal ligament-alveolar bone (PDL-AB) biointerface microtissue model using 3D bioprinting technology. This model accurately recapitulates the connection between the PDL fibroblast layer and the mineralized bone layer, maintain high cell viability, and can be used for disease mechanism research and drug screening, thereby providing an important platform for personalized periodontal tissue engineering[97] . On the other hand, 3D bioprinting is also advancing towards functional tissue construction and repair, even exploring scaffold-free strategies. By fusing spheroids derived from anterior cruciate ligament and bone-derived mesenchymal stem cells, modular multicellular microtissues were constructed.

These microtissues spontaneously formed gradient-like ligamentous, fibrocartilaginous, and bone-like regions, achieving critical de novo fibrocartilage formation while supporting external mechanical stimulation. This scalable, scaffold-free platform of heterologous cell spheroids not only provides an in vitro model for studying the mechanobiology of entheses but also demonstrates immense translational potential for developing injectable or bioprintable building blocks for enthesis repair[98] (Fig 7. A-C). Collectively, these advancements highlight the profound applications and expansive development prospects of 3D bioprinting in osteoligamentous enthesis research, spanning from precise modeling to constructing regenerative tissues.

Compared with the other interface types, bone–ligament engineering is at an earlier translational stage and is more heterogeneous in purpose. Some studies mainly serve as in vitro disease or mechanobiology models, such as periodontal ligament–alveolar bone microtissues, and are therefore valuable for mechanistic analysis, drug testing, and personalized modeling rather than immediate implantation. Others, especially spheroid-fusion or scaffold-free enthesis systems, aim to provide building blocks for future regenerative therapy, but they still require stronger evidence of mechanical durability and long-term integration before clinical use.

Structurally, ligament-related strategies overlap with tendon-to-bone approaches in their reliance on graded architecture and enthesis-like transitions; however, the ligament field has not yet achieved the same level of functional validation in animal repair models. This suggests that the current emphasis should remain on biomimetic modeling, early enthesis formation, and mechanical conditioning. For clinical translation, the most promising systems will likely be those that can combine regional differentiation with load-responsive maturation while retaining sufficient durability under cyclic stress.

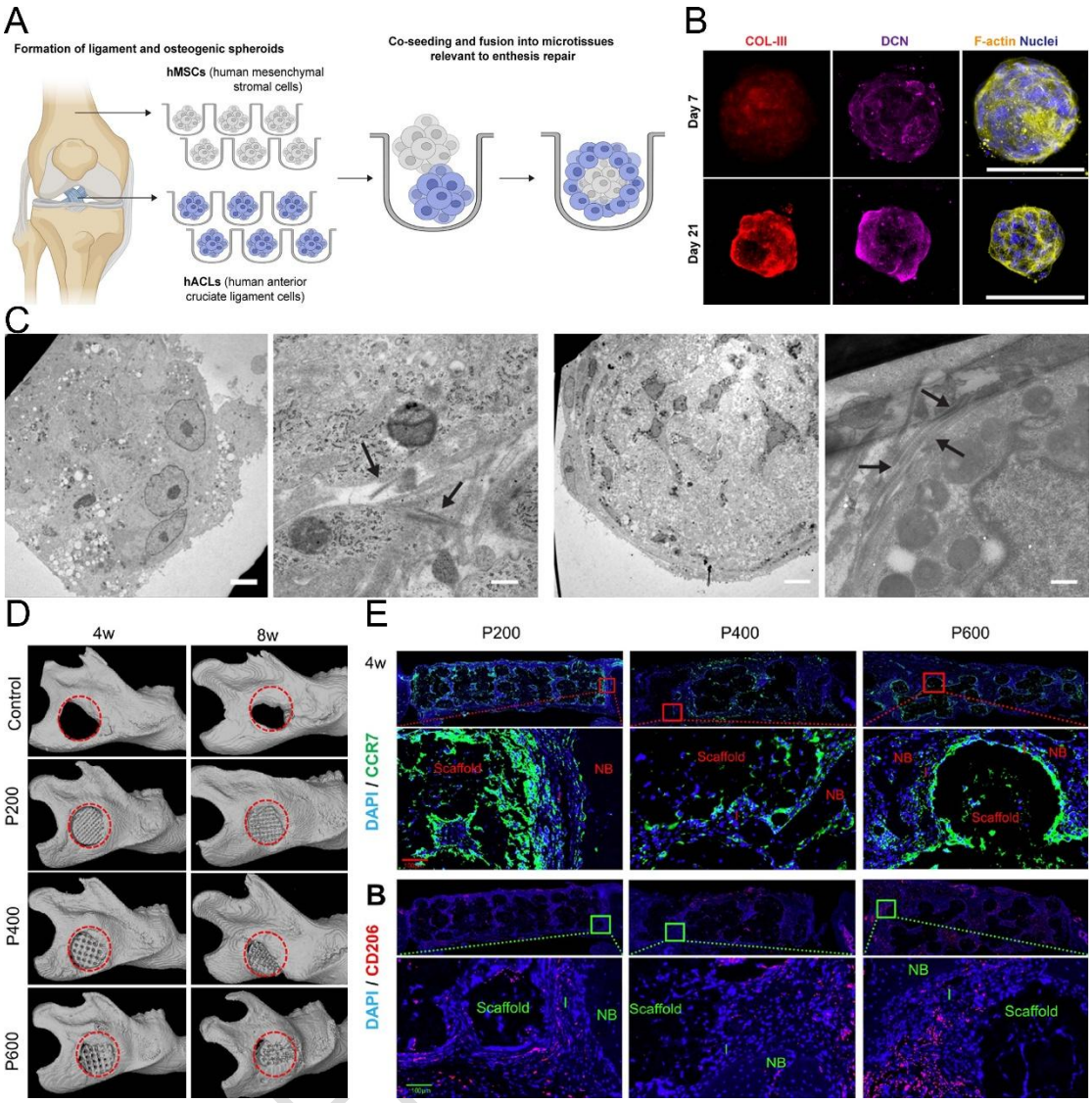

Figure 7. 3D bioprinting is used for bone-ligament and bone-immune interface regeneration. A. By co-assembling the patient-derived ACL cells and hMSCs into ligament-like and osteogenic spheres, they were fused within 10 days to form engineered micro-tissues with core-shell structure and expression of early insertion markers. B. Confocal fluorescence images showed the distribution of extracellular matrix components in ACL spheroids on day 7 (upper) and day 21 (lower). The spheres were labeled as type III collagen (red). core protein (purple), F-actin (yellow) and nucleus (blue). TEM images of L7-B15 and L7-B21 aggregates show the overall morphology of the micro-tissue and the details of the collagen fibers marked by arrows in the fusion area, with scales of 5 μm (panorama) and 500 nm (local magnification), respectively. Reprinted with permission from Giacomini et al.[98]. Copyright © 2026, ELSEVIER. D. Micro-CT three-dimensional reconstruction showed that the scaffolds in the P600 group showed more significant new bone formation than the P200 and P400 groups at 4 and 8 weeks. E. mmunofluorescence staining confirmed that the group recruited fewer M1 pro-inflammatory macrophages and more M2 anti-inflammatory macrophages at 4 weeks, indicating that the large-diameter scaffold promoted the effective regeneration of bone tissue by optimizing the immune microenvironment. Reprinted with permission from Li et al.[94]. Copyright © 2022， AMER CHEMICAL SOC.

3.7 Cross-interface comparison of design requirements in bone-tissue bioprinting

Although bone–cartilage, bone–tendon/ligament, bone–vascular, and bone–nerve interfaces are all transitional tissues, their design requirements differ substantially because each interface serves a distinct biomechanical and biological function (Table 3.). Bone–cartilage interfaces require a pronounced gradient in stiffness and mineral content, together with suppression of vascular invasion in the cartilaginous zone to preserve the avascular phenotype and prevent inappropriate endochondral ossification. Accordingly, osteochondral constructs often emphasize biphasic or zonal architectures, mineralized bone-facing regions, and cartilage-mimetic hydrogel compartments, with additional use of hypoxia, growth-factor patterning, or pore-size control to guide region-specific chondrogenic and osteogenic differentiation (**Table S1**).

In contrast, bone–tendon and bone–ligament interfaces must dissipate tensile load across a mechanically graded enthesis and avoid stress concentration at the insertion site. Therefore, these constructs prioritize composition and stiffness gradients, aligned fibrous architectures, and spatially controlled delivery of tenogenic, chondrogenic, and osteogenic cues. Compared with osteochondral interfaces, vascularization is still relevant but not usually the dominant design driver; instead, long-term mechanical integration and enthesis remodeling are central. Multilayer, coaxial, and core-shell printing strategies are particularly suitable for reproducing this hierarchical load-transfer zone.

Bone–vascular interfaces are fundamentally different because their key challenge is not simply interfacial matching but the creation of perfusable and stable microvascular networks that can sustain cell survival in large or thick bone constructs. Thus, these systems typically emphasize porosity control, interconnected channels, osteon-like architectures, and prevascularization with endothelial cells or vasculogenic co-cultures. Here, mechanical gradients are important but usually secondary to vascular continuity, lumen stability, and angiogenic maturation. Bioactive signals such as VEGF, silicate ions, and angiogenic cell–cell crosstalk are often integrated to accelerate vessel

formation and coupling with osteogenesis.

Bone–nerve interfaces require yet another design logic. Their primary goal is to support neurogenic ingrowth and neuro-osteogenic crosstalk while maintaining sufficient mechanical stability for bone repair. As a result, these constructs frequently combine conductive or piezoelectric elements, neurotrophic factors such as NGF, Schwann cells, neural stem cells, or sensory neurons, and bioactive signals that regulate CGRP-mediated osteogenesis or sympathetic modulation. Compared with bone–vascular systems, the essential requirement is not perfusion alone but the coordinated regulation of innervation, vascularization, and osteogenesis. Overall, a major challenge across all interfaces is that the dominant design priority changes from mechanical matching, to vascular supply, to neural signaling, depending on the target tissue pair.

This cross-interface comparison highlights that no single bioprinting strategy is universally optimal. Instead, interface-specific design must integrate local mechanics, cell composition, transport requirements, and biochemical signaling to reproduce the native tissue hierarchy (**Table S2**).

Table 3. Cross-interface comparison of major design requirements in 3D bioprinting for bone-tissue interface regeneration

Interface type	Dominant mechanical requirement	Vascularization requirement	Typical cell composition	Key bioactive signaling	Preferred design strategy	Main biological goal
Bone–cartilage	Strong stiffness and mineral gradients; cartilage zone should remain compliant	Low in cartilage zone; vascular invasion should be restricted	Chondrocytes, ACPCs, ADMSCs, BMSCs	Hypoxia, miRNA, HAp-related osteogenic cues	Biphasic, zonal, graded, or multilayer constructs	Maintain cartilage phenotype while enabling bone formation
Bone–tendon/ligament	Smooth tensile load transfer; high enthesis toughness; composition and stiffness gradients	Moderate; helpful for healing but not primary driver	Tenocytes, ligament fibroblasts, MSCs, TSPCs, hUCMSCs	BMP-2, growth-factor gradients, dECM cues	Coaxial, core-shell, multilayer, graded scaffolds	Regenerate functional enthesis and prevent stress concentration
Bone–vascular	Structural stability with open, perfusable channels	Very high; perfusion and microvascular maturation are central	hMSCs, ASCs, HUVECs, EPCs	VEGF, silicate ions, angiogenic co-culture cues	Osteon-like, microchannel, dual-ink, coaxial, prevascularized constructs	Enable nutrient delivery and sustain thick bone regeneration
Bone–nerve	Mechanical stability with support for neural guidance	Moderate; often coupled with vascularization	BMSCs, Schwann cells, neural stem cells, DRG neurons, PC12 cells	NGF, CGRP-related signaling, exosomes, piezoelectric or conductive cues	Multicellular, neuro-bone co-patterned, piezoelectric, in situ signaling systems	Promote innervation and neuro-osteogenic crosstalk

Abbreviations: ACPCs: Articular cartilage progenitor cells; ADMSCs: Adipose-derived mesenchymal stem cells; ASCs: Adipose-derived stem cells; BMSCs: Bone marrow-derived mesenchymal stem cells; BMP-2: Bone morphogenetic protein-2; CGRP: Calcitonin gene-related peptide; dECM: Decellularized extracellular matrix; DRG: Dorsal root ganglion; EPCs: Endothelial progenitor cells; HAp: Hydroxyapatite; hMSCs: Human mesenchymal stem cells; hUCMSCs: Human umbilical cord-derived mesenchymal stem cells; HUVECs: Human umbilical vein endothelial cells; miRNA: MicroRNA; MSCs: Mesenchymal stem cells; NGF: Nerve growth factor; TSPCs: Tendon stem/progenitor cells; VEGF: Vascular endothelial growth factor.

4. Challenges and Future Perspectives

4.1 Outstanding biological and biomechanical challenges

Three fundamental scientific limitations currently constrain the clinical translation of bioprinted bone-tissue interfaces. The first is the insufficient depth and speed of vascularization and innervation within large constructs. Most published studies demonstrate vascular and neural ingrowth in vitro or in small animal defects, but in clinically relevant large defects, cells in the construct core remain beyond the effective diffusion limit and experience progressive hypoxia, and existing microchannel designs still fall far short of the perfusion efficiency of native Haversian canal networks. Moreover, most studies quantify vascular and neural presence through immunohistochemical markers rather than functional perfusion, barrier integrity, or sensorimotor recovery, which obscures whether documented ingrowth contributes meaningfully to tissue function. The second limitation concerns the temporal control of immune regulation. Although scaffold pore size and bioactive molecules such as aptamers or metal-organic frameworks can modulate macrophage polarization in vitro and in short-term animal studies, the in vivo immune response is a dynamically evolving spatiotemporal process, and achieving an orderly transition from early moderate pro-inflammatory to late anti-inflammatory states across different patient backgrounds and healing conditions still lacks a mature design paradigm, with most studies limited to observation windows of 4–12 weeks. The third limitation is the unpredictability of mechanical integration, particularly at tendon-to-bone and ligament-to-bone interfaces, where the degradation curve of the scaffold frequently mismatches the mechanical maturation curve of newly formed tissue, creating a vulnerability window in which load-bearing capacity declines before the regenerated tissue has reached sufficient strength; long-term studies beyond six months and testing under physiologically relevant cyclic loading are still scarce. These bottlenecks reflect the fact that structural mimicry alone is insufficient and that synchronizing structure, biology, and remodeling kinetics remains the central unresolved challenge.

4.2 Practical translational and manufacturing barriers

Beyond biological bottlenecks, the transition of bioprinted bone-tissue interface constructs toward clinical use is confronted by a series of practical, yet equally decisive, manufacturing and regulatory obstacles that are rarely addressed in the academic literature. Manufacturing reproducibility remains a major concern: most published constructs are produced in small laboratory batches, and batch-to-batch variations in bioink rheology, crosslinking efficiency, post-printing cell viability (typically 40–85% depending on the printing modality), and pore architecture are seldom quantified, while the absence of standardized printer calibration, nozzle maintenance, and process validation protocols makes multicenter reproducibility and regulatory-grade quality control difficult to achieve. Cell source standardization is another unresolved issue, as the field employs heterogeneous cell populations including bone marrow- and adipose-derived MSCs, iPSCs, and primary cells with divergent proliferation kinetics, differentiation propensities, and paracrine profiles, and there is no consensus on passage number, seeding density, viability thresholds, or cryopreservation conditions, nor a validated end-to-end workflow for autologous cell expansion within clinically feasible timeframes. Long-term safety data are equally limited: most biocompatibility assessments extend only to 12 weeks, and the chronic foreign body response, the leaching of unreacted photoinitiators, uncrosslinked oligomers, and degradation products, and the potential off-target systemic effects of embedded growth factors or nanoparticles (e.g., aberrant angiogenesis) have not been systematically evaluated, with ISO 10993-series testing rarely reported. Sterile production and storage pose additional constraints: constructs containing living cells cannot withstand conventional terminal sterilization methods such as ethylene oxide, gamma irradiation, or autoclaving, and the alternatives, including aseptic cleanroom manufacturing or terminal cold sterilization, are either costly or not yet validated for complex three-dimensional structures; similarly, fresh cell-laden constructs have a shelf life of only hours to days, and validated cryopreservation protocols that preserve both scaffold architecture and post-thaw cell viability remain underdeveloped, raising unresolved questions about transport logistics, cold-chain management, and quality control between the

manufacturing site and the operating room. Together, these practical barriers—rather than biological efficacy alone—will determine whether bioprinted interface constructs can progress from proof-of-concept to reproducible, safe, and economically viable clinical products.

4.3 Future directions

Looking forward, several directions hold promise for overcoming the challenges above, provided they are pursued with realistic expectations about validation levels. Integrating bioprinting with microfluidic organ-on-chip technology can construct highly biomimetic bone-tissue interface models in vitro for high-throughput drug screening, disease mechanism research, and personalized therapeutic testing, thereby accelerating the transition from laboratory discovery to preclinical evaluation. Artificial intelligence and machine learning, trained on accumulated bioprinting datasets, may enable big data-driven optimization of bioink formulations, adaptive regulation of printing parameters, and "one-click" personalized scaffold design based on patient imaging, potentially reducing the empirical trial-and-error burden of current fabrication. In situ bioprinting, using robot-assisted or handheld devices to deposit cell- and growth factor-laden materials directly at surgical defect sites, could eliminate prolonged in vitro culture periods, secondary transplantation injury, and storage-transport constraints, although its clinical implementation will require rigorous sterility assurance and real-time quality monitoring. Finally, drawing on developmental biology, organoid-inspired and self-organizing strategies aim to design constructs that contain sufficient mechanical, biochemical, and morphogenetic cues to self-organize and self-mature in vivo rather than relying on static pre-designed architectures, which may improve robustness to manufacturing variability and patient heterogeneity. Each of these directions, however, will only contribute to clinical translation if pursued in parallel with standardized large animal validation, functional outcome assessment, and resolution of the manufacturing, safety, and regulatory issues outlined above. We anticipate that with sustained and coordinated effort, 3D bioprinting can transition from an intellectually compelling research platform toward clinically meaningful application

in the coming decade.

5. Conclusion

This review synthesizes recent advancements in 3D bioprinting technology for bone-tissue interface regeneration, encompassing both anatomically-defined interfaces (bone-cartilage, bone-tendon, bone-ligament) and functional biological interactions (bone-immune, bone-vascular, bone-nerve). The comparative framework presented across Section 3 reveals that 3D bioprinting offers a unique capacity to construct hierarchical, multifunctional scaffolds that recapitulate the complex gradients of natural interfaces. While significant progress has been made in designing biomimetic structures and incorporating bioactive cues to direct cell fate, the clinical translatability of these strategies remains largely at the stage of preclinical investigation. Evidence from the literature indicates that osteochondral and tendon-to-bone interfaces have achieved the most substantial in vivo validation in small and some large animal models, supporting continued preclinical development. However, for bone-vascular, bone-nerve, bone-ligament, and bone-immune constructs, most findings remain at the in vitro or small animal proof-of-concept stages, requiring extensive further research before clinical application can be considered. The successful translation of 3D bioprinting from laboratory promise to clinical reality will fundamentally depend on overcoming persistent biological bottlenecks, including insufficient vascularization and innervation in large constructs, inadequate temporal control of immune responses, and unpredictable mechanical integration.

Acknowledgments

None.

Funding

None.

Conflict of interest

The authors declare that they have no known competing financial interests or personal relationships that could have appeared to influence the work reported in this paper.

Author contributions

Conceptualization: Xiangran Cui, Pan Xue
Visualization: Wei Wei, Zhaoyu Liang
Writing–original draft: Tingting Zhou, Shixuan Wang
Writing–review & editing: Xiangran Cui, Shixuan Wang

Ethics approval and consent to participate

Not applicable.

Consent for publication

Not applicable.

Availability of data

Not applicable.

References

1. Pedret C, Peña-Amaro J, Balius R, Järvinen T. Histological Definition of Skeletal Muscle Injury: A Guide to Nomenclature Along the Connective Tissue Sheath/Structure. *Sports Med*. May 2025;55(5):1061-1065. doi:10.1007/s40279-024-02165-3

2. Liu L, Zhou N, Fu SN, et al. Endothelial cell-derived exosomes trigger a positive feedback loop in osteogenesis-angiogenesis coupling via up-regulating zinc finger and BTB domain containing 16 in bone marrow mesenchymal stem cell. *J Nanobiotechnol*. Nov 19 2024;22(1)721. doi:10.1186/s12951-024-03002-5

3. Yu CH, Chen RJ, Chen JL, et al. Enhancing tendon-bone integration and healing with advanced multi-layer nanofiber-reinforced 3D scaffolds for acellular tendon complexes. *Mater Today Bio*. Jun 2024;26101099. doi:10.1016/j.mtbio.2024.101099

4. Cheng C, Chaaban M, Born G, et al. Repair of a Rat Mandibular Bone Defect by Hypertrophic Cartilage Grafts Engineered From Human Fractionated Adipose Tissue. *Front Bioeng Biotechnol*. Mar 8 2022;10841690. doi:10.3389/fbioe.2022.841690

5. Liu G, Zhou WZ, Wu LA, et al. Biomimetic Construction of a Biphasic Scaffold with Hierarchical Porous Structures and Topographical Interfaces for Osteochondral Repair. *ACS Appl Mater Interfaces*. Apr 22 2026;18(15):21776-21790. doi:10.1021/acsami.6c00337

6. Bianchi E, Faccendini A, Del Favero E, et al. Topographical and Compositional Gradient Tubular Scaffold for Bone to Tendon Interface Regeneration. *Pharmaceutics*. Oct 2022;14(10)2153. doi:10.3390/pharmaceutics14102153
7. Lin T, Li JY, Luo LC, et al. VEGF-sustained regulation and hydrogel-activated graded porous titanium scaffold for functional regeneration of the tendon-bone interface. *Mater Today Bio*. Apr 2026;37102903. doi:10.1016/j.mtbio.2026.102903
8. Chen J, Zhang QY, Tan J, et al. Enhanced fibrocartilage regeneration at the tendon-bone interface injury through extracellular matrix hydrogel laden with bFGF-overexpressing human urine-derived stem cells. *Chem Eng J*. Oct 1 2024;497154333. doi:10.1016/j.cej.2024.154333
9. Shirai Y, Okano J, Nakagawa T, et al. Bone marrow-derived vasculogenesis leads to scarless regeneration in deep wounds with periosteal defects. *Sci Rep*. Nov 29 2022;12(1)doi:10.1038/s41598-022-24957-1
10. Fontana G, Nemke B, Lu Y, et al. Local delivery of TGF-(31-mRNA decreases fibrosis in osteochondral defects. *Bioact Mater*. Mar 2025;45:509-519. doi:10.1016/j.bioactmat.2024.11.033
11. Gao H, Pan Q, Dong WQ, Yao YC. Progress in Osteochondral Regeneration with Engineering Strategies. *Ann Biomed Eng*. Oct 2022;50(10):1232-1242. doi:10.1007/s10439-022-03060-6
12. Damerau A, Buttgereit F, Gaber T. Optimization of a Tricalcium Phosphate-Based Bone Model Using Cell-Sheet Technology to Simulate Bone Disorders. *Processes*. Mar 2022;10(3)550. doi:10.3390/pr10030550
13. Qiu Y, Yu B, Jiang CC, et al. Bone marrow mesenchymal stem cells overexpressing FGF-2 loaded onto a decellularized extracellular matrix hydrogel for the treatment of osteoarthritis. *Biomater Sci*. Jan 6 2026;14(1):9-30. doi:10.1039/d5bm00920k
14. Mlachkova A, Dosseva-Panova V, Ivanov I, Parvanov D, Maynalovska H. Application of platelet rich fibrin in surgical periodontal therapy: a con-trolled clinical trial. *Journal of Imab*. Oct-Dec 2022;28(4):4634-4639. doi:10.5272/jimab.2022284.4634
15. Xue NN, Ding XF, Huang RZ, et al. Bone Tissue Engineering in the Treatment of Bone Defects. *Pharmaceuticals*. Jul 2022;15(7)879. doi:10.3390/ph15070879
16. Dec P, Modrzejewski A, Pawlik A. Existing and Novel Biomaterials for Bone Tissue Engineering. *Int J Mol Sci*. Jan 2023;24(1)529. doi:10.3390/ijms24010529
17. Xu H, Cui YT, Tian YH, et al. Nanoparticle-Based Drug Delivery Systems for Enhancing Bone Regeneration. *ACS Biomater Sci Eng*. Feb 12 2024;10(3):1302-1322. doi:10.1021/acsbiomaterials.3c01643
18. Jalandhra GK, Kilian KA. Biofabrication approaches to fabricating gradients and interfaces in osteochondral tissue engineering. *Curr Opin Biomed Eng*. Sep 2024;31100544. doi:10.1016/j.cobme.2024.100544
19. Khalak FA, Decuyper JM, Khalak KA, Alonso SR, Saenz-del-Burgo L, Muñoz JLP. 3D bioprinting approaches for musculoskeletal interfaces in tissue engineering. *Int J Pharm*. Sep 15 2025;682125939. doi:10.1016/j.ijpharm.2025.125939
20. Wang YF, Chen C, Zhang CY, et al. 3D bioprinting for tendon-bone interface regeneration. *International Journal of Bioprinting*. 2025 2025;11(2):164-183. doi:10.36922/ijb.8411
21. Golebiowska AA, Nukavarapu SP. Bio-inspired zonal-structured matrices for bone-cartilage interface engineering. *Biofabrication*. Apr 1 2022;14(2)025016. doi:10.1088/1758-5090/ac5413
22. Wang YX, Hou YH, Vyas C, Huang BY, Bartolo P. An integrated hybrid 3D bioprinting of heterogeneous and zone-specific construct resembling structural and biofunctional properties of

osteochondral tissue. *Materials Futures*. Jun 1 2025;4(2)025401. doi:10.1088/2752-5724/adb7f6

23. Hu CW, Wang CM, Bian SQ, et al. In situ bioprinting: Tailored printing strategies for regenerative medicine. *International Journal of Bioprinting*. 2024 2024;10(5)3366. doi:10.36922/ijb.3366

24. Jiang XP, Kong YF, Kuss M, et al. 3D bioprinting of multilayered scaffolds with spatially differentiated ADMSCs for rotator cuff tendon-to-bone interface regeneration. *Appl Mater Today*. Jun 2022;27101510. doi:10.1016/j.apmt.2022.101510

25. Yu XG, Gholipourmalekabadi M, Wang XD, Yuan CY, Lin KL. Three-dimensional bioprinting biphasic multicellular living scaffold facilitates osteochondral defect regeneration. *Interdiscip Mater*. Sep 2024;3(5):738-756. doi:10.1002/idm2.12181

26. Senturk E, Bilici C, Afghah F, et al. 3D bioprinting of tyramine modified hydrogels under visible light for osteochondral interface. *Biofabrication*. Jul 1 2023;15(3)034102. doi:10.1088/1758-5090/acd6bf

27. Usseglio N, Santos AG, Ferrer AF, Flores J, Nieto D. High-fidelity 'top-down' DLP bioprinting of multi-material soft tissue constructs enabled by computer vision-based layer control. *Biofabrication*. Jun 1 2026;18(2)025018. doi:10.1088/1758-5090/ae55cc

28. Yang K, Lee D, Lee KH, et al. 3D-bioprinted bone scaffolds incorporating SR1 nanoparticles enhance blood vessel regeneration in rat calvarial defects. *International Journal of Bioprinting*. 2024 2024;10(3)1931. doi:10.36922/ijb.1931

29. Bedell ML, Wang ZW, Hogan KJ, et al. The effect of multi-material architecture on the ex vivo osteochondral integration of bioprinted constructs. *Acta Biomater*. Jan 1 2023;155:99-112. doi:10.1016/j.actbio.2022.11.014

30. Hu QX, Wang YH, Song YT, Liu SH, Zhang HG. Engineering triple-layer gelatin methacryloyl-alginate osteochondral construct with biomimetic curved architecture using a multi-axial, multi-process, multi-material 3D bioprinting system. *Int J Biol Macromol*. Oct 2025;327147541. doi:10.1016/j.ijbiomac.2025.147541

31. Yao K, Guo K, Wang HR, Zheng XF. Multi-Nozzles 3D Bioprinting Collagen/Thermoplastic Elasto-Mer Scaffold with Interconnect Pores. *Micromachines*. Apr 2 2025;16(4)429. doi:10.3390/mi16040429

32. Jang TS, Park SJ, Lee JE, et al. Topography-Supported Nanoarchitectonics of Hybrid Scaffold for Systematically Modulated Bone Regeneration and Remodeling. *Adv Funct Mater*. Dec 2022;32(51)2206863. doi:10.1002/adfm.202206863

33. Kim YH, Kanczler JM, Lanham S, et al. Biofabrication of nanocomposite-based scaffolds containing human bone extracellular matrix for the differentiation of skeletal stem and progenitor cells. *Bio-Des Manuf*. Mar 2024;7(2):121-136. doi:10.1007/s42242-023-00265-z

34. Kumar P, Sharma J, Kumar R, et al. Genetic and bioactive functionalization of bioinks for 3D bioprinting. *Bioprocess Biosyst Eng*. Sep 2025;48(9):1421-1449. doi:10.1007/s00449-025-03180-y

35. Wang PL, Wang T, Xu Y, Song N, Zhang X. 3D-bioprinted cell-laden hydrogel with anti-inflammatory and anti-bacterial activities for tracheal cartilage regeneration and restoration. *International Journal of Bioprinting*. 2024 2024;10(1):160-175. doi:10.36922/ijb.0146

36. Bai YX, Wang ZJ, He XL, et al. Application of Bioactive Materials for Osteogenic Function in Bone Tissue Engineering. *Small Methods*. Aug 2024;8(8)doi:10.1002/smtd.202301283

37. Liu HY, Gong YX, Zhang KH, et al. Recent Advances in Decellularized Matrix-Derived Materials for Bioink and 3D Bioprinting. *Gels*. Mar 2023;9(3)195. doi:10.3390/gels9030195

38. Chen SS, Wang Y, Li JZ, Sun HR, Siu MFF, Tan SL. 3D-printed Mg-substituted hydroxyapatite/

gelatin methacryloyl hydrogels encapsulated with PDA@DOX particles for bone tumor therapy and bone tissue regeneration. *International Journal of Bioprinting*. 2024 2024;10(5):232-255. doi:10.36922/ijb.3526

39. Cui XR, Jiao JH, Yang LL, et al. Advanced tumor organoid bioprinting strategy for oncology research. *Mater Today Bio*. Oct 2024;28101198. doi:10.1016/j.mtbio.2024.101198

40. Cui XR, Liu DD, Lu X, et al. Advanced dECM-based bioprinting strategy for tissue regeneration. *Mater Today Adv*. Mar 2026;29100733. doi:10.1016/j.mtadv.2026.100733

41. Cui XR, Liu HF, Liu YT, et al. Tissue-specific decellularized extracellular matrix rich in collagen, glycoproteins, and proteoglycans and its applications in advanced organoid engineering: A review. *Int J Biol Macromol*. Jun 2025;315144469. doi:10.1016/j.ijbiomac.2025.144469

42. Jain P, Kathuria H, Ramakrishna S, Parab S, Pandey MM, Dubey N. In Situ Bioprinting: Process, Bioinks, and Applications. *ACS Appl Bio Mater*. Apr 10 2024;7(12):7987-8007. doi:10.1021/acsabm.3c01303

43. Wang K, Khalid M, Lv HX, Song RX. Bioactive materials and drug delivery in 3D printing for bone regeneration. *Biotechnol Bioprocess Eng*. 2026;doi:10.1007/s12257-026-00276-4

44. Zhu H, Lin ZH, Luan QF, et al. Angiogenesis-promoting composite TPMS bone tissue engineering scaffold for mandibular defect regeneration. *International Journal of Bioprinting*. 2024 2024;10(1):459-476. doi:10.36922/ijb.0153

45. Jayabal R. Nanomaterials in Regenerative Medicine: Advancing the Future of Tissue Engineering. *Regener Eng Transl Med*. 2025;doi:10.1007/s40883-025-00416-x

46. Okwuwa CC, Olunusi SO, Abutu D, Umunnawuike C, Amenaghawon A, Ighalo JO. Nanocellulose for Sustainable Tissue Engineering: Modification Strategies, Structural Insights, and Innovations for Biomedical Applications. *Biopolymers*. Mar 2026;117(2)e70086. doi:10.1002/bip.70086

47. Shen MK, Wang LL, Gao Y, et al. 3D bioprinting of in situ vascularized tissue engineered bone for repairing large segmental bone defects. *Mater Today Bio*. Dec 2022;16100382. doi:10.1016/j.mtbio.2022.100382

48. Dutta SD, Patil TV, Ganguly K, Randhawa A, Lim KT. Unraveling the potential of 3D bioprinted immunomodulatory materials for regulating macrophage polarization: State-of-the-art in bone and associated tissue regeneration. *Bioact Mater*. Oct 2023;28:284-310. doi:10.1016/j.bioactmat.2023.05.014

49. Li XR, Deng QS, Liu PL, et al. Three-dimensional printed biomimetic multilayer scaffolds coordinated with sleep-related small extracellular vesicles: A strategy for extracellular matrix homeostasis and macrophage polarization to enhance osteochondral regeneration. *View*. Apr 2024;5(2)doi:10.1002/viw.20230069

50. Yu K, Huangfu H, Qin Q, et al. Application of Bone Marrow-Derived Macrophages Combined with Bone Mesenchymal Stem Cells in Dual-Channel Three-Dimensional Bioprinting Scaffolds for Early Immune Regulation and Osteogenic Induction in Rat Calvarial Defects. *ACS Appl Mater Interfaces*. 2022;14(41):47052-47065. doi:10.1021/acsami.2c13557

51. Wang L, Sun LG, Qiu ZN, et al. Gradient hydroxyapatite nanoparticles with spatial distribution facilitate the healing of tendon-to-bone interface. *International Journal of Bioprinting*. 2025 2025;11(1):501-516. doi:10.36922/ijb.6181

52. Fan TT, Meng X, Zhuge RS, et al. Design, fabrication, and biocompatibility of 3D-printed poly(LLA-ran-PDO-ran-GA)/poly (D-lactide) composite scaffolds for bone tissue engineering. *International Journal of Bioprinting*. 2024 2024;10(6):532-543. doi:10.36922/ijb.4645

53. Wang Y, Wu SH, Kuss MA, Streube PN, Duan B. Effects of Hydroxyapatite and Hypoxia on Chondrogenesis and Hypertrophy in 3D Bioprinted ADMSC Laden Constructs. *ACS Biomater Sci Eng*. May 2017;3(5):826-835. doi:10.1021/acsbiomaterials.7b00101

54. Diloksumpan P, de Ruijter M, Castilho M, et al. Combining multi-scale 3D printing technologies to engineer reinforced hydrogel-ceramic interfaces. *Biofabrication*. Apr 2020;12(2)025014. doi:10.1088/1758-5090/ab69d9

55. Ayan B, Wu Y, Karuppagounder V, Kamal F, Ozbolat IT. Aspiration-assisted bioprinting of the osteochondral interface. *Sci Rep*. Aug 4 2020;10(1)13148. doi:10.1038/s41598-020-69960-6

56. Critchley S, Sheehy EJ, Cunniffe G, et al. 3D printing of fibre-reinforced cartilaginous templates for the regeneration of osteochondral defects. *Acta Biomater*. Sep 1 2020;113:130-143. doi:10.1016/j.actbio.2020.05.040

57. Celik N, Kim MH, Yeo M, Kamal F, Hayes DJ, Ozbolat IT. miRNA induced 3D bioprinted-heterotypic osteochondral interface. *Biofabrication*. Oct 1 2022;14(4)044104. doi:10.1088/1758-5090/ac7fbb

58. Jalandhra GK, Molley TG, Hung TT, Roohani I, Kilian KA. In situ formation of osteochondral interfaces through ?bone-ink? printing in tailored microgel suspensions. *Acta Biomater*. Jan 15 2023;156:75-87. doi:10.1016/j.actbio.2022.08.052

59. Chen HY, Gonnella G, Huang J, Di-Silvio L. Fabrication of 3D Bioprinted Bi-Phasic Scaffold for Bone-Cartilage Interface Regeneration. *Biomimetics*. Mar 2023;8(1)87. doi:10.3390/biomimetics8010087

60. Zhang YJ, Li D, Liu Y, et al. 3D-bioprinted anisotropic bicellular living hydrogels boost osteochondral regeneration via reconstruction of cartilage-bone interface. *Innovation*. Jan 8 2024;5(1)100542. doi:10.1016/j.xinn.2023.100542

61. Liu DQ, Liu JS, Zhao PC, et al. 3D Bioprinted Tissue-Engineered Bone with Enhanced Mechanical Strength and Bioactivities: Accelerating Bone Defect Repair through Sequential Immunomodulatory Properties. *Adv Healthcare Mater*. Dec 2024;13(30)doi:10.1002/adhm.202401919

62. Yang XX, Wang LL, Chen X, Ling BY, Xiao JX. Digital light processing 3D bioprinting of collagen-based gradient osteochondral scaffold for cartilage-bone regeneration. *Int J Biol Macromol*. Nov 2025;331148403. doi:10.1016/j.ijbiomac.2025.148403

63. Ding HB, Zhao CR, Hu YK, et al. Biphasic Scaffolds Functionalized with Piezoelectric Nanozymes for Osteochondral Defect Regeneration. *Adv Healthcare Mater*. May 2026;15(20)doi:10.1002/adhm.202600012

64. Choi Y, Jang W, Kang R, et al. Developmentally Inspired, Mechanical-Metabolic Dual Gradient Osteochondral Constructs Bridging Regeneration and Therapeutic Screening. *Adv Sci*. Apr 2026;13(24)doi:10.1002/advs.202516602

65. Holmes B, Bulusu K, Plesniak M, Zhang LG. A synergistic approach to the design, fabrication and evaluation of 3D printed micro and nano featured scaffolds for vascularized bone tissue repair. *Nanotechnology*. Feb 12 2016;27(6)064001. doi:10.1088/0957-4484/27/6/064001

66. Byambaa B, Annabi N, Yue K, et al. Bioprinted Osteogenic and Vasculogenic Patterns for Engineering 3D Bone Tissue. *Adv Healthcare Mater*. Aug 23 2017;6(16)1700015. doi:10.1002/adhm.201700015

67. Chen YW, Shen YF, Ho CC, et al. Osteogenic and angiogenic potentials of the cell-laden hydrogel/mussel-inspired calcium silicate complex hierarchical porous scaffold fabricated by 3D bioprinting. *Materials Science & Engineering C-Materials for Biological Applications*. Oct 1

2018;91:679-687. doi:10.1016/j.msec.2018.06.005
68. Piard C, Baker H, Kamalitdinov T, Fisher J. Bioprinted osteon-like scaffolds enhance in vivo neovascularization. *Biofabrication*. Apr 2019;11(2)025013. doi:10.1088/1758-5090/ab078a
69. Chiesa I, De Maria C, Lapomarda A, et al. Endothelial cells support osteogenesis in an in vitro vascularized bone model developed by 3D bioprinting. *Biofabrication*. Apr 2020;12(2)025013. doi:10.1088/1758-5090/ab6a1d
70. Twohig C, Helsinga M, Mansoorifar A, et al. A dual-ink 3D printing strategy to engineer pre-vascularized bone scaffolds in-vitro. *Materials Science and Engineering C-Materials for Biological Applications*. Apr 2021;123111976. doi:10.1016/j.msec.2021.111976
71. Nulty J, Freeman FE, Browe DC, et al. 3D bioprinting of prevascularised implants for the repair of critically-sized bone defects. *Acta Biomater*. May 2021;126:154-169. doi:10.1016/j.actbio.2021.03.003
72. Sun X, Jiao X, Yang X, et al. 3D bioprinting of osteon-mimetic scaffolds with hierarchical microchannels for vascularized bone tissue regeneration. *Biofabrication*. Jul 1 2022;14(3)035008. doi:10.1088/1758-5090/ac6700
73. Shahabipour F, Tavafoghi M, Aninwene GE, et al. Coaxial 3D bioprinting of tri-polymer scaffolds to improve the osteogenic and vasculogenic potential of cells in co-culture models. *J Biomed Mater Res Part A*. May 2022;110(5):1077-1089. doi:10.1002/jbm.a.37354
74. Zhang HJ, Qin C, Shi Z, et al. Bioprinting of inorganic-biomaterial/neural-stem-cell constructs for multiple tissue regeneration and functional recovery. *Natl Sci Rev*. Feb 13 2024;11(4)nwae035. doi:10.1093/nsr/nwae035
75. Ju JY, Fang HM, Jie JJ, et al. Modular living assembly of bone organoids with in situ guided vascularization. *Bioact Mater*. Oct 2026;64:510-528. doi:10.1016/j.bioactmat.2026.04.020
76. Liu XF, Gaihre B, George MN, et al. 3Dbioprinting of oligo(poly ethylene glycol fumarate) for bone and nerve tissue engineering. *J Biomed Mater Res Part A*. Jan 2021;109(1):6-17. doi:10.1002/jbm.a.37002
77. Li WT, Miao WQ, Liu YH, et al. Bioprinted Constructs that Mimic the Ossification Center Microenvironment for Targeted Innervation in Bone Regeneration. *Adv Funct Mater*. Feb 2022;32(9)2109871. doi:10.1002/adfm.202109871
78. Liu JY, Zhang B, Li L, Yin J, Fu JZ. Additive-lathe 3D bioprinting of bilayered nerve conduits incorporated with supportive cells. *Bioact Mater*. Jan 2021;6(1):219-229. doi:10.1016/j.bioactmat.2020.08.010
79. Zhang HJ, Qin C, Zhang M, et al. Calcium silicate nanowires-containing multicellular bioinks for 3D bioprinting of neural-bone constructs. *Nano Today*. Oct 2022;46101584. doi:10.1016/j.nantod.2022.101584
80. Li SK, Li ZH, Yang J, Ha Y, Zhou XJ, He CL. Inhibition of Sympathetic Activation by Delivering Calcium Channel Blockers from a 3D Printed Scaffold to Promote Bone Defect Repair. *Adv Healthcare Mater*. Aug 2022;11(16)2200785. doi:10.1002/adhm.202200785
81. Wang TC, Li WT, Zhang YX, et al. Bioprinted constructs that simulate nerve-bone crosstalk to improve microenvironment for bone repair. *Bioact Mater*. Sep 2023;27:377-393. doi:10.1016/j.bioactmat.2023.02.013
82. Guo ST, He CL. Bioprinted Scaffold Remodels the Neuromodulatory Microenvironment for Enhancing Bone Regeneration. *Adv Funct Mater*. Oct 2023;33(40)2304172. doi:10.1002/adfm.202304172
83. Qin C, Zhang HJ, Chen L, et al. Cell-Laden Scaffolds for Vascular-Innervated Bone Regeneration.

Adv Healthcare Mater. May 2023;12(13)doi:10.1002/adhm.202201923

84. Zhang X, Wang SH, Dong SO, Gu JY, Liao LQ, Zhang C. Spatially heterogeneous neuro-bone construct functionalized with NGF/ BMP-2 mimetic peptides facilitates innervated bone regeneration. *Chem Eng J*. Dec 1 2025;525170272. doi:10.1016/j.cej.2025.170272

85. Su YZ, Wang HM, Liu WX, et al. Bioinspired Engineering of Streamlined Skeletal Interoception: Neural Bioprinted Piezoelectric Scaffolds for Neuro-Vascularized Bone Regeneration. *Adv Sci*. Apr 2026;13(21)doi:10.1002/advs.202524181

86. Park SH, Choi YJ, Moon SW, et al. Three-Dimensional Bio-Printed Scaffold Sleeves With Mesenchymal Stem Cells for Enhancement of Tendon-to-Bone Healing in Anterior Cruciate Ligament Reconstruction Using Soft-Tissue Tendon Graft. *Arthroscopy-the Journal of Arthroscopic and Related Surgery*. Jan 2018;34(1):166-179. doi:10.1016/j.arthro.2017.04.016

87. Tarafder S, Brito JA, Minhas S, Effiong L, Thomopoulos S, Lee CH. In situ tissue engineering of the tendon-to-bone interface by endogenous stem/progenitor cells. *Biofabrication*. Jan 2020;12(1)015008. doi:10.1088/1758-5090/ab48ca

88. Neubauer VJ, Hüter F, Wittmann J, et al. Flow Simulation and Gradient Printing of Fluorapatite- and Cell-Loaded Recombinant Spider Silk Hydrogels. *Biomolecules*. Oct 2022;12(10)1413. doi:10.3390/biom12101413

89. Bai L, Han Q, Meng ZJ, et al. Bioprinted living tissue constructs with layer-specific, growth factor-loaded microspheres for improved enthesis healing of a rotator cuff. *Acta Biomater*. Dec 2022;154:275-289. doi:10.1016/j.actbio.2022.10.058

90. Zhang XC, Song W, Han K, et al. Three-Dimensional Bioprinting of a Structure-, Composition-, and Mechanics-Graded Biomimetic Scaffold Coated with Specific Decellularized Extracellular Matrix to Improve the Tendon-to-Bone Healing. *ACS Appl Mater Interfaces*. Jun 12 2023;15(24):28964-28980. doi:10.1021/acsami.3c03793

91. Du L, Qin C, Zhang HJ, et al. Multicellular Bioprinting of Biomimetic Inks for Tendon-to-Bone Regeneration. *Adv Sci*. Jul 2023;10(21)doi:10.1002/advs.202301309

92. Kim W, Kwon DR, Lee H, et al. 3D bioprinted multi-layered cell constructs with gradient core-shell interface for tendon-to-bone tissue regeneration. *Bioact Mater*. Jan 2025;43:471-490. doi:10.1016/j.bioactmat.2024.10.002

93. Kim W, Lee SC, Lee H, et al. Bioprinted Collagen Cell Constructs with Gradient BMP-2-Loaded Microbeads for Rotator Cuff Tear Regeneration. *Adv Healthcare Mater*. Feb 2026;15(6)doi:10.1002/adhm.202504150

94. Li WF, Dai F, Zhang S, et al. Pore Size of 3D-Printed Polycaprolactone/Polyethylene Glycol/Hydroxyapatite Scaffolds Affects Bone Regeneration by Modulating Macrophage Polarization and the Foreign Body Response. *ACS Appl Mater Interfaces*. May 11 2022;14(18):20693-20707. doi:10.1021/acsami.2c02001

95. Zhou LQ, Zhang CC, Shi TB, et al. Functionalized 3D-printed GelMA/Laponite hydrogel scaffold promotes BMSCs recruitment through osteoimmunomodulatory enhance osteogenic via AMPK/mTOR signaling pathway. *Mater Today Bio*. Dec 2024;29101261. doi:10.1016/j.mtbio.2024.101261

96. Yu SY, Wu T, Xu KH, et al. 3D bioprinted biomimetic MOF-functionalized hydrogel scaffolds for bone regeneration: Synergistic osteogenesis and osteoimmunomodulation. *Mater Today Bio*. Jun 2025;32101740. doi:10.1016/j.mtbio.2025.101740

97. Vurat MT, Seker S, Lalegül-Ülker O, Parmaksiz M, Elçin AE, Elçin YM. Development of a multicellular 3D-bioprinted microtissue model of human periodontal ligament-alveolar bone biointerface:

Towards a pre-clinical model of periodontal diseases and personalized periodontal tissue engineering. *Genes & Diseases*. Jul 2022;9(4):1008-1023. doi:10.1016/j.gendis.2020.11.011

98. Giacomini F, Anand S, Vermeulen S, et al. Multicellular microtissues from fused ligament- and bone-cell spheroids relevant to enthesis repair. *Mater Today Bio*. Jun 2026;38103129. doi:10.1016/j.mtbio.2026.103129

99. Li JF, Fischer P. Advances in extrusion-based bioprinting enabled by advanced printhead and nozzle designs. *Mater Today Bio*. Apr 2026;37102941. doi:10.1016/j.mtbio.2026.102941

100. Li XR, Zheng FY, Wang XD, et al. Biomaterial inks for extrusion-based 3D bioprinting: Property, classification, modification, and selection. *International Journal of Bioprinting*. 2023 2023;9(2)649. doi:10.18063/ijb.v9i2.649

101. Lovászi B, Szucs D, Monostori T, Kemény L, Veréb Z. 3D-bioprinted bone for regenerative medicine: Current concepts and future perspectives. *International Journal of Bioprinting*. 2024 2024;10(3):141-171. doi:10.36922/ijb.2056

102. Mendoza-Cerezo L, Rodríguez-Rego JM, Macías-García A, Díaz-Prado SM, Marcos-Romero AC. Process-optimized gelatin methacryloyl-konjac glucomannan dual-network hydrogels for stable and reproducible extrusion-based 3D bioprinting. *Int J Biol Macromol*. Apr 2026;353151279. doi:10.1016/j.ijbiomac.2026.151279

103. Sakai S, Kotani T, Harada R, et al. Development of phenol-grafted polyglucuronic acid and its application to extrusion-based bioprinting inks. *Carbohydr Polym*. Feb 1 2022;277118820. doi:10.1016/j.carbpol.2021.118820

104. Zhou SY, Han CY, Ni ZJ, Yang C, Ni YH, Lv Y. Gelatin-Oxidized Nanocellulose Hydrogels Suitable for Extrusion-Based 3D Bioprinting. *Processes*. Nov 2022;10(11)2216. doi:10.3390/pr10112216

105. Lee J, Lee H. Sacrificial-Rotating Rod-Based 3D Bioprinting Technique for the Development of an In Vitro Cardiovascular Model. *Journal of Functional Biomaterials*. Jan 2024;15(1)2. doi:10.3390/jfb15010002

106. Seymour AJ, Westerfield AD, Cornelius VC, Skylar-Scott MA, Heilshorn SC. Bioprinted microvasculature: progressing from structure to function. *Biofabrication*. Apr 1 2022;14(2)022002. doi:10.1088/1758-5090/ac4fb5

107. Li BW, Wang Z, Huang CZ, et al. A comprehensive review on the printing efficiency, precision, and cell viability in 3D bioprinting. *Med Eng Phys*. Nov 2025;145104448. doi:10.1016/j.medengphy.2025.104448

108. Lombardi L, Scalzone A, Ausilio C, Gentile P, Tammaro D. Optimizing nozzle design in extrusion-based 3D bioprinting to minimize mechanical stress and enhance cell viability. *International Journal of Bioprinting*. 2025;11(4):315-327. doi:10.36922/ijb025190182

109. Garna DF, Zhang ZT, Di-Silvio L. hBM-MSC-Laden 3D Bioprinted Gelatin-Alginate Hydrogels: Physicochemical Characterisation and Osteogenic Lineage Commitment. *Gels*. May 1 2026;12(5)387. doi:10.3390/gels12050387

110. Zhang H, Cong Y, Osi AR, et al. Direct 3D Printed Biomimetic Scaffolds Based on Hydrogel Microparticles for Cell Spheroid Growth. *Adv Funct Mater*. Mar 2020;30(13)1910573. doi:10.1002/adfm.201910573

111. Bera AK, Ghosh S, Ghosh A, et al. Directional biofabrication using collagen-based decellularized extracellular matrix bioink for multi-layered cellular alignment in tissue constructs. *Int J Biol Macromol*. Nov 2025;331148449. doi:10.1016/j.ijbiomac.2025.148449

112. Ghahri T, Salehi Z, Aghajanpour S, et al. Development of osteon-like scaffold-cell construct by

quadruple coaxial extrusion-based 3D bioprinting of nanocomposite hydrogel. *Biomater Adv*. Feb 2023;145213254. doi:10.1016/j.bioadv.2022.213254

113. Azhar M, Malviya R, Balusamy B, et al. Hybrid bioprinting platforms: integrating microfluidic, AI, and additive manufacturing for functional tissue constructs. *Adv Compos Hybrid Mater*. Apr 11 2026;9(3)231. doi:10.1007/s42114-026-01780-0

114. Colosi C, Shin SR, Manoharan V, et al. Microfl uidic Bioprinting of Heterogeneous 3D Tissue Constructs Using Low-Viscosity Bioink. *Adv Mater*. Jan 27 2016;28(4):677-684. doi:10.1002/adma.201503310

115. Costantini M, Colosi C, Swieszkowski W, Barbetta A. Co-axial wet-spinning in 3D bioprinting: state of the art and future perspective of microfluidic integration. *Biofabrication*. Jan 2019;11(1)012001. doi:10.1088/1758-5090/aae605

116. Li H, Li NN, Zhang H, et al. Three-Dimensional Bioprinting of Perfusable Hierarchical Microchannels with Alginate and Silk Fibroin Double Cross-linked Network. *3D Print Addit Manuf*. Apr 1 2020;7(2):78-84. doi:10.1089/3dp.2019.0115

117. Diaz RS, De-Juan-Pardo EM, Dalton PD, Dargaville TR. Semi-Woven Structures via Dual Nozzle Melt Electrowriting. *Macromol Mater Eng*. Apr 2023;308(4)doi:10.1002/mame.202200526

118. Kola I, Joshi JS, Mpofu NS, Ehrmann A. 3D biomaterials produced by near-field electrospinning and melt electrowriting. *Hemijska Industrija*. 2025;79(4):209-217. doi:10.2298/hemind250111013k

119. Paxton NC, Daley R, Forrestal DP, Allenby MC, Woodruff MA. Auxetic tubular scaffolds via melt electrowriting. *Mater Des*. Aug 2020;193108787. doi:10.1016/j.matdes.2020.108787

120. Daneshfar A, Dumee LF, Hughes TC, Kong LX. Thermally-stable photo-curing chemistry for additive manufacturing by direct melt electrowriting. *Addit Manuf*. Mar 2022;51102623. doi:10.1016/j.addma.2022.102623

121. Liu EI, Footner E, Quigley A, et al. A Versatile Method to Create Perfusable, Capillary-Scale Channels in Cell-Laden Hydrogels Using Melt Electrowriting. *Macromol Mater Eng*. Sep 2023;308(9)doi:10.1002/mame.202300042

122. Jian YL, Dehli F, Wisbar M, Taoum A, Campos DD. In situ bioprinting: bioprinting methods, bioinks, cell sources & advanced bioprinting strategies. *Biofabrication*. Mar 1 2026;18(1)012007. doi:10.1088/1758-5090/ae3cc3

123. Singh S, Choudhury D, Yu F, Mironov V, Naing MW. In situ bioprinting - Bioprinting from benchside to bedside? *Acta Biomater*. Jan 1 2020;101:14-25. doi:10.1016/j.actbio.2019.08.045

124. Yang YY, Yu ZY, Lu XH, et al. Minimally invasive bioprinting for in situ liver regeneration. *Bioact Mater*. Aug 2023;26:465-477. doi:10.1016/j.bioactmat.2023.03.011

125. Kim GJ, Kim L, Kwon OS. Application of 3D Bioprinting Technology for Tissue Regeneration, Drug Evaluation, and Drug Delivery. *Applied Science and Convergence Technology*. Jan 2023;32(1):1-6. doi:10.5757/asct.2023.32.1.1

126. Shabbir M, Kim GJ, Kwon OS. Advances in the application of biofabrication: 3D bioprinting of living materials. *Appl Phys Rev*. Jun 2026;13(2)021324. doi:10.1063/5.0310643

127. Liu JC, Shahriar M, Xu HQ, Xu CX. Cell-laden bioink circulation-assisted inkjet-based bioprinting to mitigate cell sedimentation and aggregation. *Biofabrication*. Oct 1 2022;14(4)045020. doi:10.1088/1758-5090/ac8fb7

128. Liu JC, Xu HQ, Shahriar M, Xu CX. Modeling of cell distribution dynamics in cell-laden bioink with active circulation. *Addit Manuf*. Jul 5 2023;73103669. doi:10.1016/j.addma.2023.103669

129. Ng WL, Huang X, Shkolnikov V, Suntornnond R, Yeong WY. Polyvinylpyrrolidone-based bioink:

influence of bioink properties on printing performance and cell proliferation during inkjet-based bioprinting. *Bio-Des Manuf*. Nov 2023;6(6):676-690. doi:10.1007/s42242-023-00245-3
130. Li XD, Liu BX, Pei B, et al. Inkjet Bioprinting of Biomaterials. *Chem Rev*. Oct 14 2020;120(19):10596-10636. doi:10.1021/acs.chemrev.0c00008
131. Zhu W, Ma XY, Gou ML, Mei DQ, Zhang K, Chen SC. 3D printing of functional biomaterials for tissue engineering. *Curr Opin Biotechnol*. Aug 2016;40:103-112. doi:10.1016/j.copbio.2016.03.014
132. Choudary R, Saini N, Chopra DS, Singh D, Singh N. A comprehensive review of 3D bioprinting biomaterials: Properties, strategies and wound healing application. *J Mater Res*. Jul 14 2023;38(13):3264-3300. doi:10.1557/s43578-023-01078-7
133. Kirbus B, Brachmann E, Hengst C, Menzel S. Additive manufacturing of 96 MHz surface acoustic wave devices by means of superfine inkjet printing. *Smart Mater Struct*. Jul 2018;27(7)075042. doi:10.1088/1361-665X/aac629
134. Liu C, Pandit PP, Parsons C, Khan F, Hu YB. Acoustic field-assisted inkjet-based additive manufacturing of carbon fiber-reinforced polydimethylsiloxane composites. *J Manuf Processes*. Aug 2022;80:87-94. doi:10.1016/j.jmapro.2022.05.059
135. Ghosh E, Rego GP, Ghosh RN, et al. Advances in In Situ Bioprinting: A Focus on Extrusion and Inkjet-Based Bioprinting Techniques. *Regener Eng Transl Med*. 2025;doi:10.1007/s40883-025-00420-1
136. Guerra A, Fortunato GM, Batoni E, Vozzi G, De Maria C. Multi-material and multi-scale platform for robotic based in situ bioprinting. *Results Eng*. Mar 2025;25104219. doi:10.1016/j.rineng.2025.104219
137. Prabhu A, Nandagopal MSG, Yegneswaran PP, Singhal HR, Mani NK. Inkjet printing of paraffin on paper allows low-cost point-of-care diagnostics for pathogenic fungi. *Cellulose*. Sep 2020;27(13):7691-7701. doi:10.1007/s10570-020-03314-3
138. Ghazali HS, Askari E, Ghazali ZS, Naghib SM, Braschler T. Lithography-based 3D printed hydrogels: From bioresin designing to biomedical application. *Colloid Interface Sci Commun*. Sep 2022;50100667. doi:10.1016/j.colcom.2022.100667
139. Zhang XQ, Zhang X, Li Y, Zhang YX. Applications of Light-Based 3D Bioprinting and Photoactive Biomaterials for Tissue Engineering. *Materials*. Dec 2023;16(23)7461. doi:10.3390/ma16237461
140. Wu LF, Zhao JJ, Huang JW, Huang PF, Zhao HY. Advances and challenges in three-dimensional bioprinting of bone organoids: Materials, techniques, and functionalization strategies. *International Journal of Bioprinting*. 2025;11(5):025190183. doi:10.36922/ijb025190183
141. Müller M, Becher J, Schnabelrauch M, Zenobi-Wong M. Printing Thermoresponsive Reverse Molds for the Creation of Patterned Two-component Hydrogels for 3D Cell Culture. *Jove-Journal of Visualized Experiments*. Jul 2013;(77)e50632. doi:10.3791/50632
142. Soliman BG, Major GS, Atienza-Roca P, et al. Development and Characterization of Gelatin-Norbornene Bioink to Understand the Interplay between Physical Architecture and Micro-Capillary Formation in Biofabricated Vascularized Constructs. *Adv Healthcare Mater*. Jan 2022;11(2)2101873. doi:10.1002/adhm.202101873
143. Rizzo R, Ruetsche D, Liu H, et al. Multiscale Hybrid Fabrication: Volumetric Printing Meets Two-Photon Ablation. *Adv Mater Technol*. Jun 2023;8(11)doi:10.1002/admt.202201871
144. Vidler C, Halwes M, Collins DJ. In Situ Characterisation of Hydrogels via Dynamic Interface Printing. *Adv Sci*. May 2026;13(28)doi:10.1002/advs.202515106
145. Jeong YG, Yoo JJ, Lee SJ, Kim MS. 3D digital light process bioprinting: Cutting-edge platforms for resolution of organ fabrication. *Mater Today Bio*. Dec 2024;29101284.

doi:10.1016/j.mtbio.2024.101284
146. Li HB, Dai JL, Wang ZX, et al. Digital light processing (DLP)-based (bio)printing strategies for tissue modeling and regeneration. *Aggregate*. Apr 2023;4(2)doi:10.1002/agt2.270
147. Kühl J, Kruempelmann SM, Hildebrandt L, et al. Nanomaterial-modified bioinks for DLP-based bioprinting of bone constructs: Impact on mechanical properties and mesenchymal stem cell function. *International Journal of Bioprinting*. 2024 2024;10(6):471-495. doi:10.36922/ijb.4015
148. Rajput M, Mondal P, Yadav P, Chatterjee K. Light-based 3D bioprinting of bone tissue scaffolds with tunable mechanical properties and architecture from photocurable silk fibroin. *Int J Biol Macromol*. Mar 31 2022;202:644-656. doi:10.1016/j.ijbiomac.2022.01.081
149. Loterie D, Delrot P, Moser C. High-resolution tomographic volumetric additive manufacturing. *Nat Commun*. Feb 12 2020;11(1)852. doi:10.1038/s41467-020-14630-4
150. Pellizzon N, Seta B, Kruse CS, Salajeghe R, Spangenberg J. Investigating thermal strains and chemical shrinkage in tomographic volumetric additive manufacturing. *Addit Manuf*. May 5 2025;105104781. doi:10.1016/j.addma.2025.104781
151. Tisato S, Vera G, Song QC, Nekoonam N, Helmer D. Additive manufacturing of multi-material and hollow structures by Embedded Extrusion-Volumetric Printing. *Nat Commun*. Jul 22 2025;16(1)6730. doi:10.1038/s41467-025-62057-6
152. Dong YH, Wang D, Chen JN, Jeon TJ, Kang LF. Advances in 3D printed blood-brain barrier models. *Biofabrication*. Jun 1 2026;18(2)022006. doi:10.1088/1758-5090/ae5d73
153. Singh R, Mori N, Kida YS. Methodological innovations in perfusable vascular networks: Advancing high-density tissue models. *Regenerative Therapy*. Jun 2026;32101109. doi:10.1016/j.reth.2026.101109
154. Wang M, Zang TY, Sun XH, Cui XR, Wang N. Advanced 3D bioprinting for bone oncology research. *International Journal of Bioprinting*. 2026;12(3):026130115. doi:10.36922/ijb026130115
155. Rukavina P, Koch F, Wehrle M, et al. In vivo evaluation of bioprinted prevascularized bone tissue. *Biotechnol Bioeng*. Dec 2020;117(12):3902-3911. doi:10.1002/bit.27527